PERIODICO di MINERALOGIA
established in 1930

DIPARTIMENTO
DI SCIENZE DELLA TERRA
SAPIENZA
UNIVERSITÀ DI ROMA

An International Journal of
Mineralogy, Crystallography, Geochemistry,
Ore Deposits, Petrology, Volcanology
and applied topics on Environment, Archaeometry and Cultural Heritage

Gold metallogeny in the east of Iran

Somayeh Samiee [1], Sedigheh Zirjanizadeh [1,*], Mohammad Hassan Karimpour [2]

[1] Department of Geology, Faculty of Science, University of Gonabad, Gonabad, Iran
[2] Department of Geology and Research Center for Ore Deposit of Eastern Iran, Faculty of Science, Ferdowsi University of Mashhad, Mashhad, Iran

ARTICLE INFO

Submitted: April 2022
Accepted: September 2022
Available on line: November 2022

* Corresponding author:
szirjanizadeh@yahoo.com

Doi: 10.13133/2239-1002/17724

How to cite this article:
Samiee S. et al. (2022)
Period. Mineral. 91, 225-255

ABSTRACT

Exploration in the east of Iran (EI) led to the identification of four types of gold mineralization in nine regions, consisting IOCG-type gold deposits (Qale-Zari, Koodakan, and Kuh-e-Zar), epithermal-type (Arghash, Khunik, and Chah Shaljami), reduced intrusion-related gold system (RIRGS) types (Tarik Darreh and Hired), and mesozonal-type orogenic gold deposits (Torghabeh). The compositional diversity of porphyry intrusions in these tectono-magmatic environments generally form in volcanic arc settings except for Hired deposit that is in a syn-collision setting, with the most restricted range (different types of granitoids that are partly high-K calk-alkaline to shoshonitic) which occurred in three main episodes. They are: (1) Triassic in which Tarik-Darreh and Torghabeh deposits generated, (2) Eocene-Oligocene episode, when the Qale-Zari, Koodakan and Kuh-e-Zar, Khunik and Chah-Shaljami formed, and (3) Oligo-Miocene episode for Hired deposit. The Hired and Tarik Darreh deposits are related to the reduced ilmenite-series granitoid, whereas the other deposits are related to oxidized magnetite-series granitoids. Evaluation of tectonic setting as well as local controls strongly suggests that continued exploration in the region will lead to the identification of additional gold deposits.

Keywords: gold metallogeny; east of Iran; IOCG; epithermal; RIRGS; orogenic gold deposits.

INTRODUCTION

Historically, Iran is an important country in terms of metal deposits. The special geological setting of Iran (active and relatively young and its correspondence with active continental margins) has made it a geodynamic setting appropriate for formation of various types of deposits, particularly, gold deposits (Dahooei et al., 2016). Iran owns ~7% of global mineral resources, ranked among 15 major mineral-rich countries, nevertheless, mining sector is not well-developed. The gold deposits of Iran have formed throughout the Late Proterozoic to Quaternary times by different paragenesis events, such as magmatogenic, volcanogenic, hydrothermal, metamorphic, ophiolitic, melange-listwaenite, and placer-type. East of Iran (EI) is a unique geological area, where numerous deposits of copper (like Sarcheshmeh copper porphyry, Teknar massive sulfide copper mine, Qale-Zari copper-gold mine), lead and zinc (Mehdi Abad lead and zinc deposit), gold (Kuh-e-Zar deposit), coal (Parvadeh Tabas coal deposits) and other minerals are concentrated. This paper provides a summary on the geologic, tectonic, mineralogic, and geochemical phenomena in as much as the potential for gold mineral exploration in EI, which includes nine gold deposits (i.e., Qale-Zari, Kuh Zar, Koodakan, Arghash, Khunik, Chah Shaljami, Tarik Darreh, Hired and Torghabeh, Figure 1, Table 1). The studied area structurally involves the Lut Block (Qale-Zari, Koodakan, Khunik, Chah Shaljami, and Hired deposits), the boundary between Central Iran and Kopeh Dagh Zone (Tarik Darreh deposit), Sabzevar Zone (Arghash deposit)

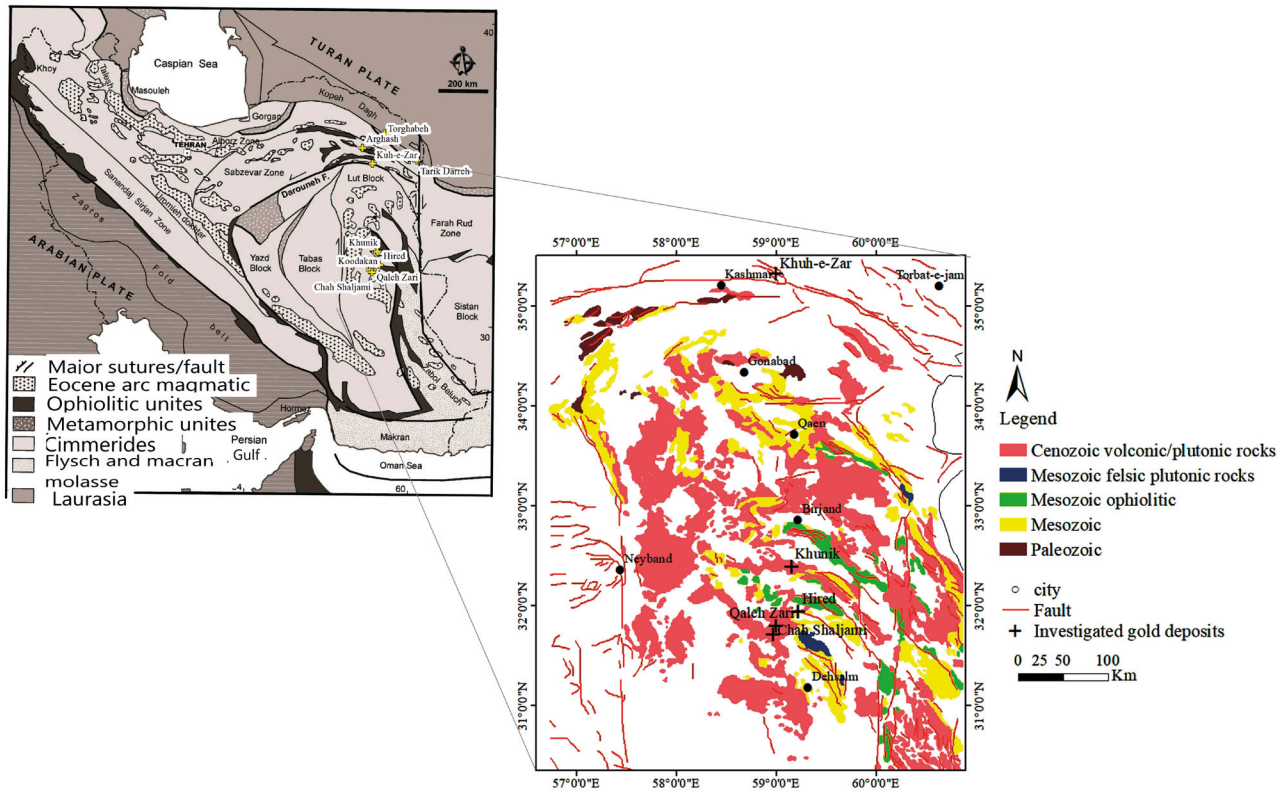

Figure 1. Distribution of investigated gold deposits in Structural Map of Iran (Alavi, 1991; Ramezani and Tucker, 2003) and simplified geology map of the Lut Block, eastern Iran (Based on maps from the Geological Survey of Iran, 1992, 2009, 1: 250,000-series maps).

and collision zone of Iran and Turan plates (Torghabeh deposit) (Figure 1). Investigation on these structural zones is necessary to understand the formation of various gold deposits in the EI. However, the Lut Block Magmatic Belt is the main metallogenic province in the EI. The Lut Block is ~900 km in length, being surrounded by the Nehbandan Fault (to the east) and the Nayband Fault (to the west, Figure 1). The rocks in the Lut block consists of Mesozoic shales and carbonates with Late Cretaceous ophiolitic belts, followed by Cenozoic volcanic and intrusive rocks and terrestrial sediments. Cenozoic magmatism in the Lut Block is widespread and consists predominantly of Eocene-Oligocene andesitic to dacitic volcanic rocks, with local subvolcanic granodioritic to granitic plutons (Figure 1, Karimpour et al., 2005). Mineral deposits in the Eastern Iran are related to the magmatism of Tertiary age. Gold mineralization in the Lut Block is associated with mineralization of copper, silver, lead-zinc, antimony, and tungsten and occurs in the Upper Triassic-Jurassic volcanic-sedimentary rock successions and in Tertiary volcanics (Figure 1, Richards et al., 2012; Karimpour et al., 2005). Qale-Zari, Hired, Chah Kalap, Shourab, Chah Zaghoo, and Khunik comprise the gold deposits and indications of the Lut Block (Table 1) (Ghorbani, 2002; Ghorbani, 2008a; Karimpour et al., 2005; Samiee, 2015). Kopeh Dagh Basin is situated in the northeast of Iran (Figure 1). The Torbat-e-Jam granitoid stock in the Kopeh Dagh Zone is the main magmatism in this region of Middle-Upper Triassic age. This garnitoid stock intruded into metasedimentary rocks and metallogeny of the Kopeh Dagh was primarily created by this garnitoid intrusion. The Sabzevar Zone is located between the Jovain and the Doruneh faults (Figure 1), which is overlain by Paleozoic sediments, Upper Cretaceous ophiolitic melange and Tertiary magmatic rocks (Omrani, 2018a; Omrani et al., 2018b). Arghash deposit in the northwest of Iran is located at the rim of the Sabzevar Structural Zone (Figure 1).

The geology and mineralization of typical gold deposits in the EI have been articulated by many authors (Karimpour et al., 2005; Karimpour, 2005; Mohammadi, 2006; Karimpour et al., 2007; Samiee and Zirjanizadeh, 2019; Amraie and Niroumand, 2014; Karimpour et al., 2017 NE Iran. The prevailing stratigraphic unit is composed of Cenozoic volcanic rocks (rhyolitic to andesitic in composition; Mazloumi et al., 2008; Alaminia et al., 2013; Afsharpour et al., 2007, 2012; Malekzadeh

Table 1. Significant geological characteristics of some important gold deposits in Iran.

N.	Deposit/ prospective area	Geographic coordinates	Host rocks	Genetic type	Age of mineralization	Gold-related ore minerals	Resource (t)/ Grade (g/t)	Data source
1	**Muteh**	E50°45′00″/ N33°42′00″	Felsic schist and metarhyolite	Orogenic, Intrusion related (?)	Eocene	Pyrite, chalcopyrite, arsenopyrite, pyrrhotite, sphalerite, bismutite	14 t @ 3 g/t Au	Rashidnejad Omran (2002); Moritz et al. (2006); Kouhestani et al. (2008, 2014)
2	**Zartorosht**	E57°10′00″/ N28°12′00″	Mafic to intermediate volcanic-pyroclastic rocks	Orogenic	Tertiary	Pyrite, chalcopyrite, galena, sphalerite, arsenopyrite, pyrrhotite	17.2 g/t Au	Rastgoo Moghadam et al. (2008)
3	**Qolqoleh**	E46°06′08″/ N36°08′08″	Andesite to andesitic basalt, metavolcanic rocks and sericite schist	Orogenic	Upper Cretaceous-Tertiary	Pyrite, chalcopyrite, pyrrhotite, sphalerite	Up to 3 Mt @ 3.5 g/t Au	Aliyari et al. (2007, 2008, 2009)
4	**Kervian**	E46°06′00″/ N36°08′00″	Felsic to mafic metavolcanic and metasedimentary rocks	Orogenic	Upper Cretaceous-Tertiary	Pyrite, chalcopyrite, arsenopyrite, realgar	-	Heidari (2004), Heidari et al. (2006)
5	**Qabaqloujeh**	E46°06′59″/ N36°05′35″	Metavolcanic phyllite, schist and mylonitic	Orogenic	Upper Cretaceous-Tertiary	Pyrite, chalcopyrite, arsenopyrite	1 Mt @ 1 g/t Au	Nosratpoor (2008)
6	**Kharapeh**	E45°15′51″/ N36°42′23″	Limestone, contact between andesite dyke and limestone	Orogenic	Upper Cretaceous-Tertiary	Pyrite, chalcopyrite, galena, sphalerite	70,000 t @ 1.52 g/t Au	Niroumand et al. (2011)
7	**Alut**	E45°52′49″/ N36°10′50″	Mafic to intermediate volcanic rocks, sericite and biotite schist and granite	Orogenic	Upper Cretaceous-Tertiary	Pyrite, chalcopyrite, sphalerite, pyrrhotite	0.1-52 g/t Au	Tajeddin et al. (2006)
8	**Torghabeh**	E59°25′00″/ N36°20′00″	Tonalite- granodiorite and slate	Mesosonal orogenic	Early Mesozoic	Pyrrhotite, arsenopyrite, gold, pyrite, galena	0.5-5 g/t Au	Karimpour et al. (2006)
9	**Barika**	E36°11′16″/ N45°39′03″	Metaandesite and tuff	Au-rich massive sulfide	Lower Cretaceous-Tertiary	Electrum, sphalerite, pyrite, galena, tetrahedrite, tennantite, chalcopyrite	Average 0.5 to 5 g/t Au	Tajeddin et al. (2004, 2006)
10	**Astaneh**	E49°25′50″/ N33°52′30″	Granite, Granodiorite intrusion and microgranodiorite dykes	Intrusion related	Early to late Eocene	Chalcopyrite, pyrite, arsenopyrite, pyrrhotite, sphalerite, marcasite, bismuth	1-2.5 g/t Au	Nezafati (2006), Nekouvaght Tak (2008)

Table 1. ...Continued

N.	Deposit/ prospective area	Geographic coordinates	Host rocks	Genetic type	Age of mineralization	Gold-related ore minerals	Resource (t)/ Grade (g/t)	Data source
11	**Agdarreh**		Reefal limestone	Carlin-type	Miocene	Pyrite, sphalerite, galena, sulphides, sulphosalts, tellurides and native bismuth,	24.5 t @ 3.7 g/t Au	Daliran (2008)
12	**Zarshuran**	E46°-48°/ N36°-37°	Black shale limestone and dolomite	Carlin- type	Miocene	Pyrrhotite, pyrite, chalcopyrite; base metal sulphides, arsenical pyrite; orpiment, realgar, stibnite	27 Mt @ 4 g/t Au	Mehrabi et al. (1999); Asadi et al. (2000)
13	**Sheikh-Ali**	E56°46′20″/ N24°09′00″	limestones and embedded by the pillow basaltic lavas	Cyprus-type (Ophiolite-hosted) VMS deposit	Upper Cretaceous	Pyrite, chalcopyrite, sphalerite, specularite	0.64 t. @75 g/t	Rastad et al., 2002
14	**Chah Zard**	E48°3′36″/ N31°5′48.56″	Andesitic to rhyolitic volcanic	Epithermal	late Miocene	pyrite, marcasite, arsenian pyrite, arsenopyrite, chalcopyrite, sphalerite, galena, gold (in electrum and native form), and silver sulfosalts.	~2.5 Mt @12.7 g/t Ag and 1.7 g/t Au	Kouhestani (2011); Kouhestani et al. (2012, 2015, 2017)
15	**Sharafabad - Hizeh Jan**	E45°- 48°/ N38°-39°	Pyroclastic, volcanic rocks	Epithermal	Oligocene-Miocene	Pyrrhotite, pyrite, cobanite, chalcopyrite, galena, sphalerite and gold	2.3 t. @ average 4 g/t Au	Nakhjevani (2005)
16	**Golouje**	E54°21′09″/ N37°05′13″	Rhyodacite, trachyandesite, dacite	Epithermal	Oligocene	Galen, sphalerite, chalcopyrite, pyrite	2237018 t. @ average 1.85 g/t Au	Taqilua et al. (2011)
17	**Khunik**	E59°10′28″/N 32°23′08″	Granitoids, subvolcanic rocks	Epithermal	Eocene	Pyrite, magnetite, chalcopyrite	0.3-4280 mg/t Au	Samiee et al. (2019)
18	**Chah Shaljami**	E58°-59°/ N31°-32°	Granodiorite porphyry	Epithermal	Eocene	Galena, chalcopyrite, molybdenite, magnetite, pyrite, enargite, arsenopyrite	0.3 g/t Au	Arjmandzadeh et al. (2011)
19	**Arghash**	E58°38′22″/ N35°54′10″	Granite and volcanic rocks	Epithermal	Late Eocene	Pyrite, arsenopyrite, chalcopyrite, galena	0.3-3.2 g/t Au	Alaminia et al. (2013)
20	**Chah Paleng**	E54°11′/ N32°57′	Shale, sandstone (Shemshak Formation)	W (Cu-Au) vein type	Mesozoic	Quartz, apatite, scheelite, sulfide and arsenide minerals	1-1.2 g/t Au	Ghaderi et al. (2014)

Table 1. ...Continued

N.	Deposit/ prospective area	Geographic coordinates	Host rocks	Genetic type	Age of mineralization	Gold-related ore minerals	Resource (t)/ Grade (g/t)	Data source
21	**Khuni**	E54°13′/ N32°27′	Plutonic and volcanic rocks	Epithermal	Eocene-Oligocene	Oxide mineralization low concentration of base metals	Average 475.7 ppb Au	Rasai and Heydarian Dehkordi (2012)
22	**Zaglik**	E47°4′12″/ N38°29′24″	Andesite, pyroclastic rocks	Epithermal	Oligocene	Pyrite, chalcopyrite, galena, tetrahedrite, gold	16 g/t Au	Ebrahimi et al. (2009, 2011)
23	**Agharak and Annigh**	E46°22’12”/ N38°49’12”	Granodiorite, monzonite and diorite-gabbro	Stock work and vein type	Upper Eocene to Oligocene	Pyrite, chalcopyrite	0.x% Cu, 1-2% Mo, 2 g/tAu	Ghadirzadeh (2002)
24	**Touzlar**	E47°40’12.00”/ N36°44’24”	Andesite, pyroclastic rocks	Epithermal	Lower Miocene	Pyrite, chalcopyrite, bornite	4-5 g/t Au	Heidari et al. (2015)
25	**Sarv Gunav**	E 48°4’48”/ N35°12’0.00”	Porphyritic dacite and lithic tuff	Epithermal	Paleocene	Pyrite, Arsenopyrite, realgar, orpiment, cinnabar and native gold	262 g/t Au	Richards (2003)
26	**Safi Khanloo**	E47°17’60”/ N38°24’36“	Dacite, andesite, monzogranite	Epithermal	Oligocene	Pyrite, marcasite, chalcopyrite, gold	1-10 g/t Au	Ghadimzadeh (2002)
27	**Gandi**	E54°38’/ N35°20’	A sequence of volcaniclastic (lapilli tuffs), sedimentary rocks (siltstones, sandstones) and volcanic (rhyolite to rhyodacite)	Epithermal	Middle Eocene	Native gold within oxidized pyrite (hydr)oxides (goethite) coexists with galena and chalcopyrite	5 t., average 14.5 (68.3) g/t Au, 30.6 (161) g/t Ag	Fard et al. (2006); Shamanian et al. (2004)
28	**Khuh-e-Zar**	E58°57′00″/ N35°20′00″	Volcanic and subvolcanic rocks	IOCG-type	Eocene	Specularite, hematite and gold	3.02 g/t Au	Karimpour et al. (2017)
29	**Qale- Zari**	E59°00′00″/ N31°50′00″	Andesite to andesite basalt, shale and mudstone	IOCG	Tertiary	Specularite, chalcopyrite, sulfosalts, hematite	0.5-35 g/t Au	Hassan Nejad (1993)
30	**Noghdouz**	E47°21’36”/ N38°23’24”	Alkali granite-monzogranite	IRIGS	Late Eocene	Chalcopyrite, pyrite, tetrahedrite, gold		Ghadimzadeh (2002); Miranvari et al. (2019)
31	**Tarik Darreh**	E60°42′17″/ N35°30′7″	Shale and mudstone (Miankuhi Formation)	IRIGS	Triassic	Arsenopyrite, quartz, pyrite	0.45 to 12.9 g/t Au	Ghavi et al. (2018)
32	**Hired**	E59°15′00″/ N31°54′00″	Shale, sandstone, marl, tuff, conglomerate, pyroclastic and volcanic rocks	IRIGS	Oligo-Miocene	pyrite, arsenopyrite, pyrrhotite, chalcopyrite ± galena ± sphalerite	400-5200 mg/t Au	Karimpour et al. (2012)

Table 1. ...Continued

N.	Deposit/ prospective area	Geographic coordinates	Host rocks	Genetic type	Age of mineralization	Gold-related ore minerals	Resource (t)/ Grade (g/t)	Data source
33	**Nabijan**	E46º48′/ N38º46′	monzogranite, monzogranodiorite, diorite	Skarn-porphyry	Oligocene	Pyrite and minor chalcopyrite, sphalerite and galena	320000 Mt. 37.1 g/t Au,	Shokohi (2007); Jamali et al. (2017)
34	**Bala Zard**	E59°6'0.00"/ N31°9'36.00"	Rhyolite- andesite	Epithermal	Eocene	Pyrite, chalcopyrite	2.47 g/t Au	Miri et al. (2021)
35	**Meiduk**	E 55°12'36"/ N30°24'36"	Andesite, basalt, pyroclastic rocks	Porphyry copper	Middle Miocene (12.5 Ma)	chalcopyrite, galena, magnetite, molybdenite, pyrite, sphalerite, tetrahedrite	150 Mt, 1.15% Cu	Aliani et al. (2009); Arian et al. (2011)
36	**Chahar Gonbad**	E56°18'36"/ N29°57'36"	Volcanic rocks, intrusive bodies and sedimentary rocks	Porphyry copper	Middle Eocene to Lower Miocene	Pyrite and chalcopyrite	19.24% Cu, 15.5 Au g/t, 355 g/t Ag	Yousefi and Moradian (2012)
37	**Sungun**	E46°42'36"/N 38°42'0.00"	Sediments, volcanics, quartz-monzonite porphyry	Porphyry copper	Oligocene-Miocene	Pyrite, chalcopyrite and molybdenite	850 Mt, 0.62% Cu, 0.01% Mo	Aghazadeh et al. (2015)
38	**Iju**	E54°56'56"/ N30°32'13"	Andesite, pyroclastic rocks, quartz diorite, tonalite	Porphyry copper	Eocene	Pyrite, chalcopyrite and molybdenite	25 Mt, 0.46% Cu	Talebi and Ghaderi (1384)
39	**Dalli**	E50°19'27"/ N34°16'20"	Andesite, pyroclastic rocks, granodiorite and diorite porphyry	Porphyry copper	Miocene (~17 and 21 Ma)	Chalcopyrite, pyrite, magnetite	8 Mt, 0.5% Cu, 0.75 g/t Au	Daneshjou et al. (2017)
40	**Darreh Zar**	E55°54'15"/ N29°52'55"	Andesite, basalt, trachyandesite , tuff, granodiorite and diorite porphyry	Porphyry copper	Oligocene-Miocene	Pyrite, chalcopyrite, bornite, molybdenite	475 Mt, 0.36% Cu, 0.005% Mo	Aghazadeh et al. (2015)
41	**Ali abad**	E53°50'36"/ N31°38'14"	Dacite, rhyodacitic tuff, granodiorite	Porphyry	Miocene	Chalcopyrite, chalcocite, molybdenite, galena sphalerite	0.73% Cu, 0.005% Mo, 19 g/t Au	Zarasvandi et al. (2010)
42	**Seridune**	E55°54'43.2043"/ N29°58'12"	Andesite, granodiorite	Porphyry copper	Miocene	Chalcopyrite, galena, hematite, magnetite, molybdenite, pyrite, sphalerite	0.46% Cu	Barzegar (2007)
43	**Sar Kuh**	E55°48'52"/ N29°56'9"	Volcanics, granodiorite porphyry	Porphyry copper	Miocene	Pyrite, chalcopyrite, molybdenite and magnetite	16 Mt, 0.46% Cu	Shafiei and Shahabpour (2008)

Table 1. ...Continued

N.	Deposit/ prospective area	Geographic coordinates	Host rocks	Genetic type	Age of mineralization	Gold-related ore minerals	Resource (t)/ Grade (g/t)	Data source
44	**Now Chun**	E55°51'22"/ N29°55'18"	Rhyodacite, diorite	Porphyry copper	Oligo-Miocene	Chalcopyrite, galena, hematite, magnetite, molybdenite, pyrite, sphalerite	80 Mt, 0.32% Cu	Shafiei and Shahabpour (2008)
45	**Bagh Khoshk**	E55°59'24"/ N29°49'54"	Tuff, rhyolite andesite, diorite	Porphyry copper	Oligo-Miocene	Pyrite, chalcopyrite, bornite, molybdenite, chalcocite and covellite	24 Mt, 0.27% Cu	Shafiei and Shahabpour (2008)
46	**Dar Alu**	E57°6'25"/ N29°24'55"	Granodiorite porphyry	Porphyry	Oligo-Miocene	Chalcopyrite, magnetite and pyrite	18 Mt, 0.47% Cu	Shafiei and Shahabpour (2008)
47	**Serenu**	E54°58' 59"/ N30°28'59.88"	Pyroclastics, andesite, diorite	Porphyry copper	Oligo-Miocene	chalcocite, chalcopyrite, galena, sphalerite	100 Mt, 0.5% Cu	Shafiei and Shahabpour (2008)
48	**Abdar**	E55°18'8"/ N30°18'2"	Pyroclastics, andesite, diorite	Porphyry copper	Miocene-Pliocene	Pyrite, chalcopyrite, galena, sphalerite, molybdenite	0.43% Cu, 0.009% Mo, 0.085 g/t Au	Shafiei et al. (2008); Mclnnes et al. (2003)
49	**Kahang**	E52°28'51"/ N32°55'54"	Tuff, dacite, andesite, monzodiorite	Porphyry	Oligo-Miocene	Chalcopyrite, pyrite, magnetite	40 Mt, 0.53% Cu, 0.02% Mo	Komaili et al. (2016)
50	**Miveh rood**	E46°16'12"/ 38°32'24"	Flysch sediments, sub-volcanic rocks	Epithermal-porphyry-skarn	Oligo-Miocene	Pyrite, chalcopyrite, bornite	1 ppm Au, 0.1%Cu,	Alirezaei et al. (2005)
51	**Darreh Zereshk**	E53°50'46"E/ N31°33'47"	Quartz diorite, tonalite, limestone	Porphyry	Miocene	Chalcopyrite, pyrite, chalcocite, bornite + magnetite	14-80 mg/t Au	Zarasvandi et al. (2004)
52	**Shadan**	E58°58'47"E/ N32°21'26"	Dacite, rhyodacite and quartz monzonite and granodiorite	Porphyry copper- gold	38.2 Ma	Pyrite, chalcopyrite bornite, chalcocite, pyrrhotite, magnetite, hematite, gold	0.3% Cu, 0.4 g/t Au	Mahdavi et al. (2019)
53	**Maherabad**	E59°00'23"E/ N32°30'14"	Monzonitic porphyries	Porphyry copper- gold	Middle Eocene	Pyrite, chalcopyrite, sporadic magnetite, pyrrhotite	2% Cu, 2 g/t Au	Malekzadeh and Karimpour (2011)
54	**Tannurjeh**	E58°35'60"/ N35°22'48"	Rhyolite, dacite, rhyodacite, subvolcanic rocks	Porphyry copper- gold	Oligo-Miocene	Pyrite, chalcopyrite	Au 0.1-30 g/t	Karimpour (2007)

Shafaroudi et al., 2012; Samiee, 2015; Arjmandzadeh et al., 2011; Shabani, 2010; Ghavi et al., 2018; Askari et al., 2015). Mining companies in all different regions of Iran are exploring for gold mineralization. According to these researches, we have tackled a wide range of perspectives, notably regional tectonic and geochemical features (whole rock and isotope), and mineralogic properties so as to assimilate tectonics and metallogeny of gold mineralization in the EI.

GOLD-BEARING PROVINCES OF IRAN

From the viewpoint of global tectonism, Iran is situated in the Alpine-Himalayan Tectonic Belt. The latter has been formed as a result of the closure of an ancient ocean called the Tethys. The tectonic and structural setting of Iran in the Alpine-Himalayan Orogenic Belt and its related major mineralization, have been studied by many researchers.

According to the structural-metallogenic zones and type of gold mineralization (Figure 2 and Table 1), the

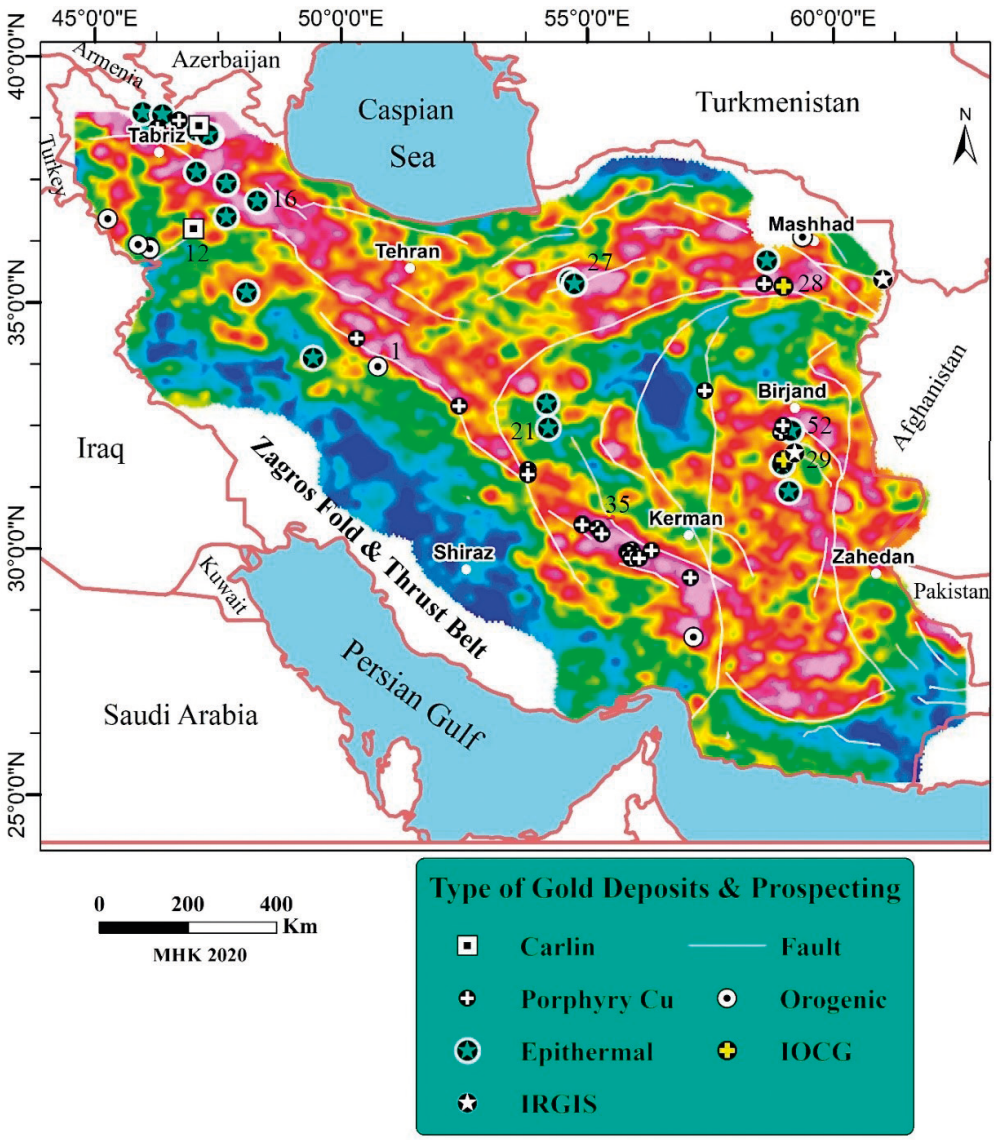

Figure 2. Distribution of some important gold deposits in Iran. Some of important deposits were marked by number based on Table 1. Data for Carlin type from Daliran, 2008, Porphyry Cu data from Daneshjou et al., 2017; Shafiei and Shahabpour, 2008; Aghazadeh et al., 2015, Epithermal type data from Shokohi, 2007; Nakhjevani, 2005; Samiee et al., 2019; Arjmandzadeh et al., 2011, data for IRGIS type from Hassan Nejad, 1993; Ghavi et al., 2018; Karimpour et al., 2012, Orogenic type from Tajeddin et al. (2006); Karimpour et al., 2006, IOCG type from Karimpour et al., 2017; Hassan Nejad, 1993.

gold-bearing provinces in Iran, are classified as shown in Figure 3 (Ghorbani, 2002; Ghorbani, 2008a and Maghsoudi et al., 2005).

TYPE AND DISTRIBUTION OF GOLD DEPOSITS IN EI

There are different globally-recognized types of gold deposits. The different deposit types are thought to have formed in a variety of geological environments over a wide range of crustal depths. They are classified base on parameters include the geological environments, host rocks, mineralization types, and hydrothermal signatures as expressed by ore and alteration, mineralogy and chemistry (e.g., Boyle, 1979; Cox and Singer, 1986; Bache, 1986; Heald et al., 1987).

The most significant mineralization types comprise gold deposits in the EI (Figure 1) viz. IOCG (in Qale-Zari, Koodakan, and Kuh-e-Zar areas), epithermal (in Arghash, Khunik, and Chah Shaljami areas), RIRGS (in Tarik-Darreh and Hired areas), and mesozonal orogenic-type (Torghabeh) gold deposits.

IOCG (Iron oxide copper gold deposits)

In the EI, IOCG deposits consist of Qale-Zari and Kuh-e-Zar mines.

Qale-Zari specularite rich Cu-Au-Ag deposit

The Qale-Zari mine is located 180 km south of Birjand (Figure 1). The lithology of the Qale-Zari deposit comprises Jurassic sandstones and shales (the oldest rocks exposed in the Qale-Zari area), volcanic rocks, and gabbro-dioritic intrusions (host the veins of mineralization). Some subvolcanic rocks (Eocene in age) have intruded into the volcanic rocks (Figure 4, Karimpour et al., 2005; Mohammadi, 2008). The composition of volcanic rocks is andesite to andesite-basalt and sub-volcanic rocks are quartz monzonite, monzonite, monzodiorite and diorite. Andesite from the western region of Qale-Zari was dated 40.5±2 Ma. (Kluyer et al., 1978).

Based on Omidianfar et al. (2020), the crystallization age of intrusions in the Qale- Zari deposit is 38 to 41 Ma.

Alteration, mineralization and geochemistry

Propylitic alteration assemblages are very widespread in the Qale-Zari area due to the presence of epidote and chlorite as secondary minerals. Argillic alteration is locally present. Silicification is mainly found within a zone adjacent to the veins. Mineralization in this area is controlled by faults. The entire mineralized zone is ~4 km. Three major sub-parallel quartz veins are being mined. Veins are, in general, very steep, dipping 70-90º NE.

The intrusions (monzogabbro and monzodiorite to diorite) and volcanic rocks host the veins (Figure 4, Karimpour et al., 2005). Quartz is the most common constituent in all veins in the Qale-Zari mine. Specularite is the most abundant oxide after quartz (up to 25%), and chalcopyrite, pyrite, gold, galena with several types of sulfosalt minerals are the other ore minerals at the Qale-Zari deposit. Mineralization can be divided into four stages based on cross-cutting relationship and temperatures of ore-forming fluid (see Karimpour et al., 2005). Based on Karimpour et al. (2005), temperature of homogenization of primary fluid inclusions in quartz associated with specularite and Cu, Ag, and Au mineralization was between 240 °C and 360 °C. The salinity of ore fluid was between 1.0 and 6.0 wt% eq. NaCl and the CO_2 were <0.1 mole%. Ore grade at Qale- Zari deposit is 2 to 9% Cu, 100 to 650 ppm Ag, and 0.5 to 35 ppm Au.

Koodakan copper-gold vein type deposit

Koodakan area, 180 Km south of Birjand, is located in the central part of the Lut Block (Figure 1). Koodakan area is located in the north of Qale-Zari mine, and, in fact, comprises the continuation of Qale-Zari mineralization type.

In the study area, rock units include Tertiary volcanic, intrusive, sub-volcanic, and pyroclastic rocks (Figure 5).

The rocks units in this area are composed of granodiorite, dioritic dikes, andesite and andesite-basalt. Volcanic rocks are extended over the study area and are mainly affected by various intensities of propylitic and/or carbonate alteration. Volcanic rocks are mainly andesitic in composition (Samiee and Zirjanizadeh, 2019).

Alteration, mineralization and geochemistry

Propylitic alteration is the dominant alteration in the Koodakan area. Argillic alteration is locally present within surface outcrops. Silicification is mainly cropped out both adjacent to mineralized veins, and to a lesser amount as pervasive silica.

Mineralization occurs as vein-type and is mainly controlled by a system of faults and joints and hosted by pyroclastic units (especially agglomerate) or occurs in the contact between agglomerate and andesitic rocks. Three styles of veins identified at the area consist of: 1) quartz + specularite + chalcopyrite ± galena ± pyrite veins; 2) quartz + Fe-oxides (limonite) veins. 3) The NW-SE-trending carbonate veins mainly occurred in northern parts of the study area. These veins do not contain any ore minerals (Samiee and Zirjanizadeh, 2019). Thermometric analysis of fluid inclusions shows that temperature of mineralization is between 109 °C to 429 °C and salinity is in the range of 0.9 to 2.2 wt% of NaCl eq. (Amraie and Niroumand, 2014).

The concentration of Au in mineralized veins ranges from 0.8-13.9 ppm. The content of Cu ranges from 75-9928 ppm, Pb between 7 ppm to >3%, Zn are consistent,

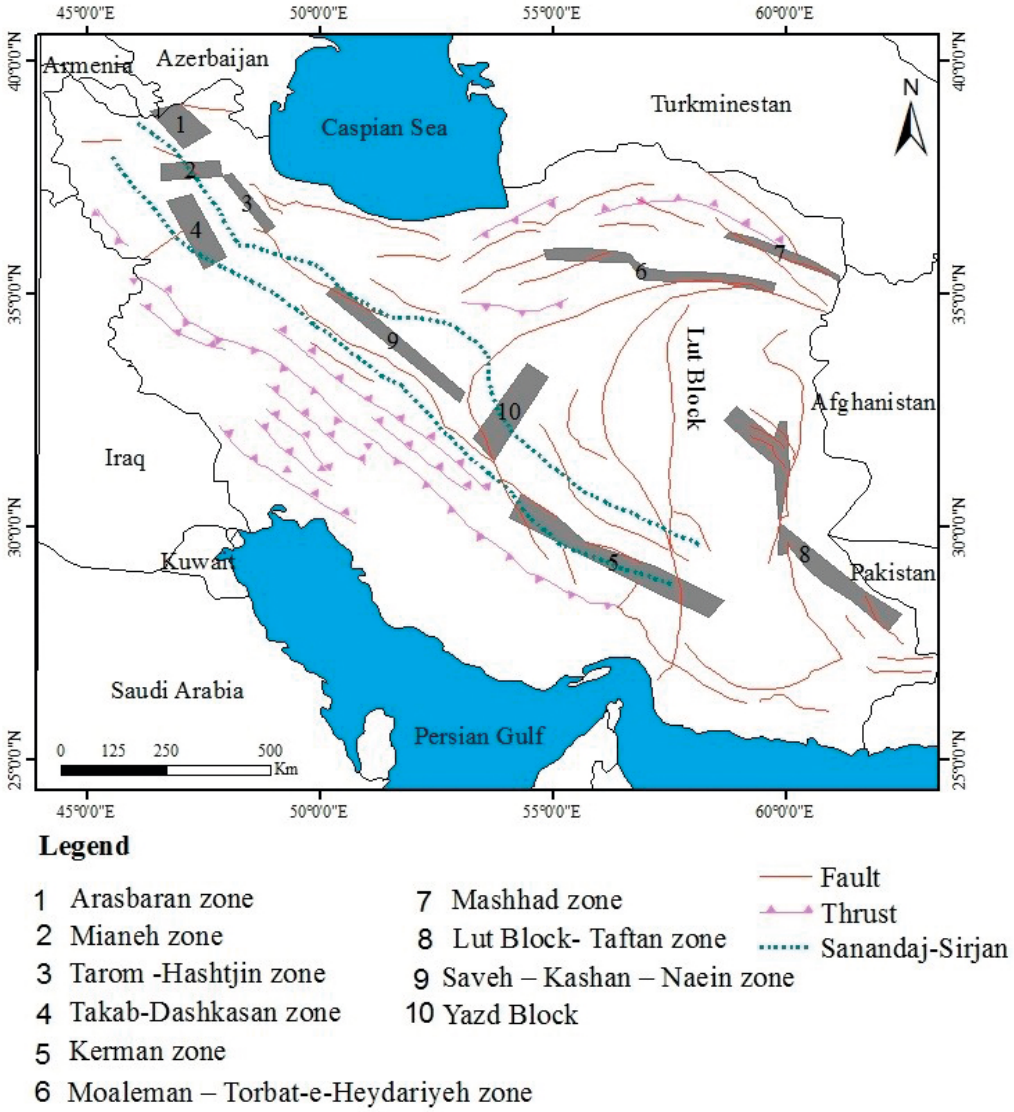

Figure 3. Gold-bearing provinces of Iran (modified after Ghorbani, 2002). 1) The Arasbaran Zone includes Songun, Masjed Daghi, Hizeh Jan, Safi Khanloo-Naghdooz and Nabi Jan (Table 1); 2) The indications of gold in the Mianeh Zone are located at Armoodagh and Aghoran (Ghorbani 2002a, 2008h ; Maghsoudi et al., 2005); 3) Some of gold indications in Tarom-Hashtjin gold-bearing Zone include Khalifeloo, Zeh-Abad, Koohiyan, Dizeh Jin, Chal, Aliabad-e Moosavi, Lak, Somagh, Bashgol, Ab Torsh, Gav Kamar, Senjedeh, Zajkan, Marshoon, Abbasabad, Rashtabad and Lohne (Ghorbani, 2002; Kouhestani et al., 2018; Kouhestani et al., 2019 a,b; Kouhestani et al., 2020; Kouhestani et al., 2022); 4) Some of gold deposits and indications in Takab-Dashkasan Zone include Zarshouran and Agdarreh (Table 1); 5) The porphyry deposits of Sarcheshmeh (Table 1) and Darreh Hamze (Jiroft) and vein deposits of Bazman, Abdar, Chah Mesi, Oroos Morghi, Chahar Gonbad, Baghdeh, and Dolat-Abad fall within the Kerman Zone (Ghorbani, 2002); 6) Examples of deposits and indications in Moaleman-Torbat-e-Heydariyeh Zone include Arghash, Gandi, Kuh Zar (Torbat-e-Heydariyeh), Kuh Zar (Damghan), Qal'e Joogh, Zar Mehr, Darestan, Kalateh Teymoor, Chah Moosa, Kakiyeh, Bid-e Mohammad Hassan, and Taknar (some of these deposits are expatiated on Table 1) (Alaminia et al., 2013, Karimpour et al., 2017); 7) Mashhad Zone contains Tarik Darreh and Torghabeh deposits (Table 1, Karimpour et al., 2006; Ghavi et al., 2018); 8) The gold deposits and indications of the Lut Block comprise: Qale-Zari, Hired, Chah Kalap, Shourab, Chah Zaghoo, and Khunik (Table 1, Karimpour et al., 2005; Samiee, 2015); 9) Some gold deposits in Saveh-Kashan-Naein gold-bearing Zone include Gorgab I and II (both skarn-type), Qal'e Sardar, Maranjab, Ghasem-Abad, Serajiyeh, Cheshme Talhe, and Kuh Dom (all are vein-type) (Ghorbani, 2002; Ghorbani, 2008a; Maghsoudi et al., 2005). 10) The gold deposits and indications of Yazd Block include Khuni, East Khuni, Anarak, Chah Mileh, Southern Chah Palang, Nadooshan, Darreh Zereshk, Chah Zard (Table 1), Torkamani, Tal Siyah, Ashin, Booteh Alam, God Morad and Gorva, (Ghorbani, 2002; Ghorbani, 2008a; Maghsoudi et al., 2005).

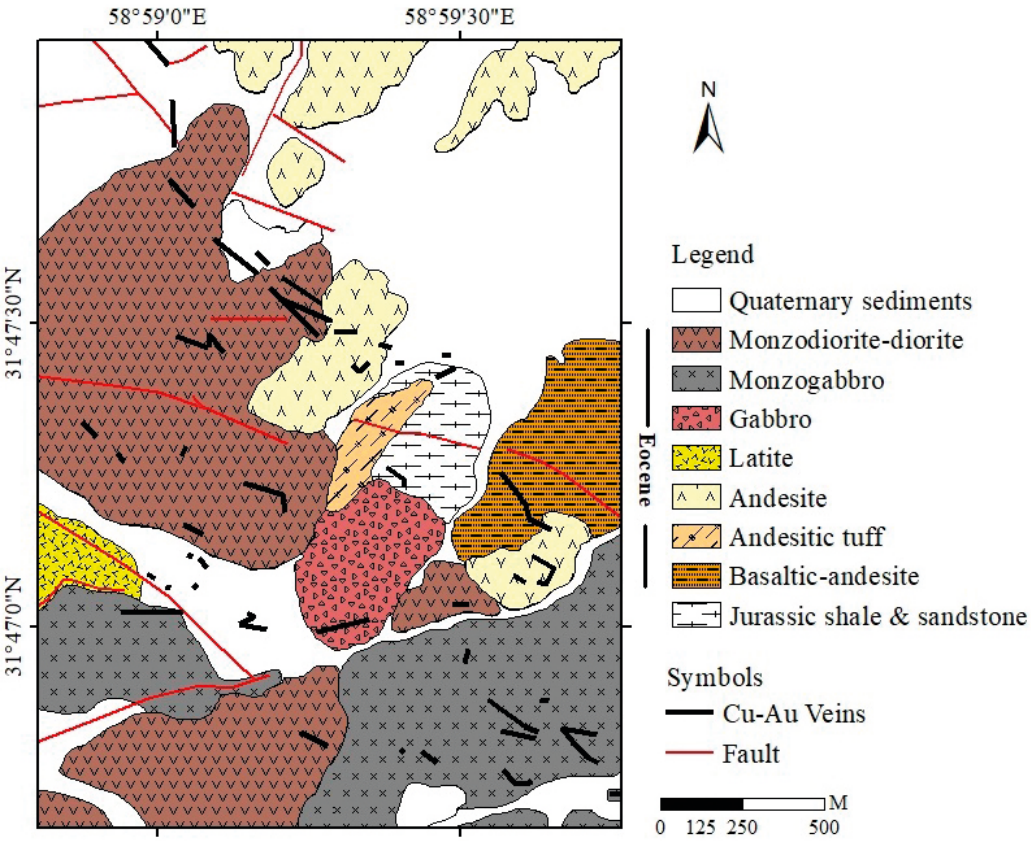

Figure 4. Geology map of the Qale-Zari area (Karimpour et al., 2005).

and range from 25 ppm to 10.928%. Arsenic represents a widespread distribution halo in studied veins and its contents varies between 5 and 424 ppm (Amraie and Niroumand, 2014).

Kuh-e-Zar specularite rich iron oxide gold deposit

The Kuh-e-Zar deposit is located in the centre of the Khaf-Kashmar-Bardaskan Magmatic Belt, approximately 40 km NW of Torbat-e-Heidarieh township (Figure 1). The major rock types in the Kuh-e-Zar deposit are Cenozoic calc alkaline volcanic rocks (rhyolitic-dacitic pyroclastic rocks, rhyolitic tuff, and latite-trachyte lava) and sub-volcanic intrusive stocks and dikes (intruded into volcanic rocks) (Figure 6). The volcanic rocks are hosts of gold mineralization in the Kuh-e-Zar deposit. Intrusive rocks spatially close to mineralization include diorite, granodiorite, quartz monzonite, quartz monzodiorite and syenogranite (Figure 6).

Mineralization, Alteration, Geochemistry

Mineralization in Kuh-e-Zar deposit occurs mainly within the volcanic rocks, and comprises several orebodies of similar alteration, mineralogy and texture. The orebodies are composed of fifteen individual major iron oxide-gold veins and several minor veins, filling fractures and faults. The ore minerals at the Kuh-e-Zar deposit are dominated by specularite and gold with small amounts of pyrite, chalcopyrite, and galena. Pyrite has disseminated in host rocks and transformed into goethite. Hematite, goethite, malachite, covellite, and cerussite are secondary minerals. The main gangue minerals include quartz, siderite, chlorite, and albite (Karimpour et al., 2017 NE Iran. The prevailing stratigraphic unit is composed of Cenozoic volcanic rocks (rhyolitic to andesitic in composition). Hydrothermal alteration includes silicification, albitization and propylitic zones. Minor sericitic-argillic zones are also observed within intrusive rocks.

Having a proven reserve of over 3 Mt of gold ore, 3 ppm Au, and with low concentrations of As, the Kuh-e-Zar represents a unique gold deposit in Iran (Mazloumi et al., 2008). Microthermometric study of fluid inclusions shows homogenization temperatures at medium-high temperature of 248 to 491 °C. Salinities of ore-forming

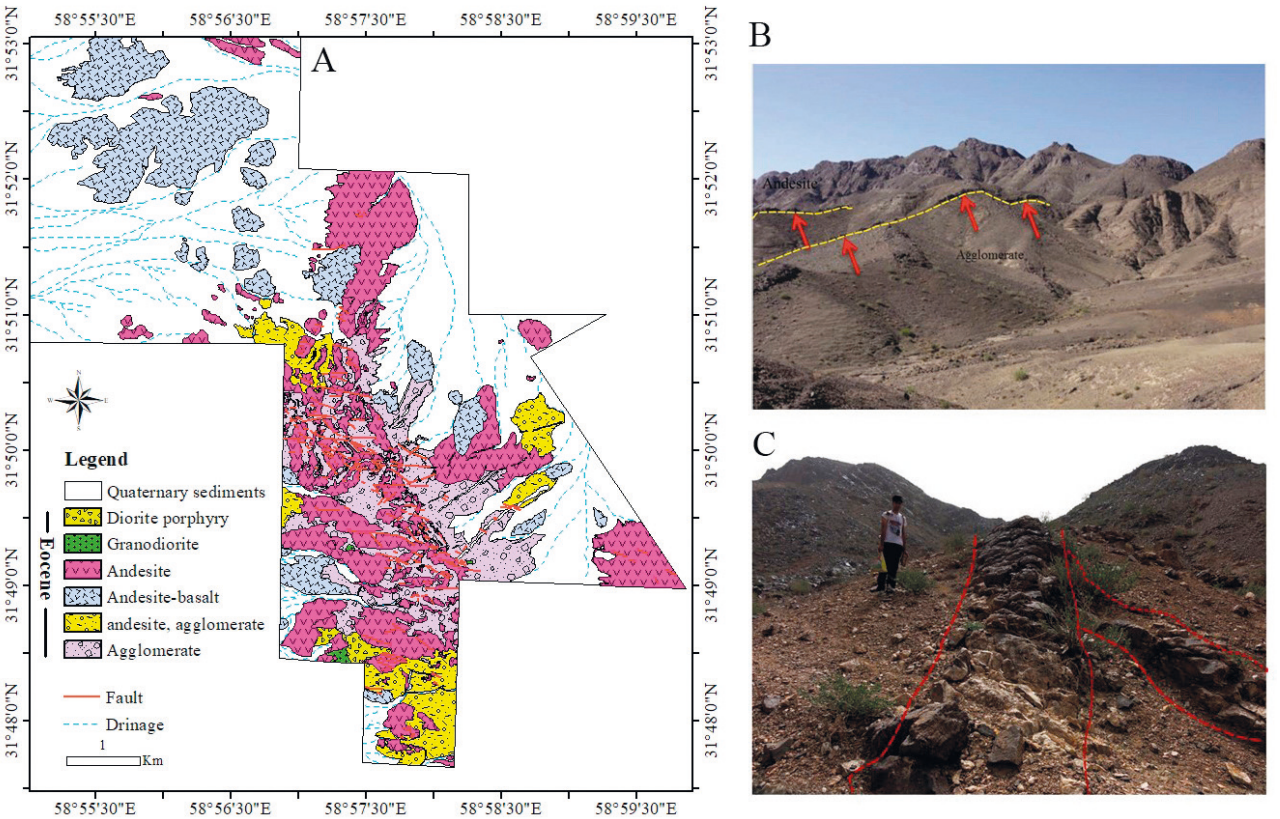

Figure 5. A) Simplified geology map of the Koodakan area; B) Outcrops of diorite porphyry dikes intruded into agglomerate units, looking to the west; C) The outcrop of the quartz + specularite + chalcopyrite ± galena ± pyrite vein in the Koodakan prospecting area, looking southeast.

fluids are medium-low, ranging from 4 to 19.2 wt% NaCl eq. (Karimpour et al., 2017). Fluid inclusions data and mineral assemblages of the Kuh-e-Zar deposit reveal that the ore-forming fluids have been medium-high temperature, medium-low salinity H_2O-NaCl system and a high oxygen fugacity.

Epithermal gold deposits

Arghash gold- antimony vein type deposit

Arghash- Ghasem-Abad deposit is located approximately 45 km southwest of Neishabur in northeastern Iran (Figure 1). The exposed rocks in the Arghash prospect area consist volcanic rocks (andesite and dacite), and plutonic rocks are mostly diorite, quartz diorite, quartz monzodiorite, granodiorite and granite with minor sedimentary rocks (limestone, sandstone and conglomerate) (Figure 7, Alaminia et al., 2013).

Based on Alaminia et al. (2013), field relationships indicate the following sequence of magmatic events (Figure 10): (1) Arghash diorite (oldest); (2) older volcanic series (includes sub-volcanic intrusions); (3) hornblende-granitoids; (4) fine-grained granite; (5) younger andesite/dacite series (pre-Oligocene); (6) stocks and dykes of quartz-monzodiorite porphyries and lamprophyres (Oligocene or younger). The status of the pillow basalts is unclear, which are tectonically intercalated with the older volcanic series.

Alteration, mineralization and geochemistry

The surface and sub-surface alteration zones which were mapped include: 1) argillic zone, 2) sericite-quartz-pyrite-calcite zone, 3) carbonate zone, 4) propylitic zone 5) silicified zone, 6) chlorite-sericite-calcite, and 7) sericite-calcite (Alaminia et al., 2013).

The mineralization is intimately associated with sericite and silicification alterations as veinlet and with propylitic zone as disseminated. Mineralized veins have mainly surrounded the lamprophyres in the south-eastern part of the area. Study area includes five gold-bearing calcite-quartz veins, Au-I to Au-V, and one antimony-rich vein (Sb) hosted by intermediate to silicic volcanic rocks, tuffs, granite, granodiorite, and Oligocene-Miocene

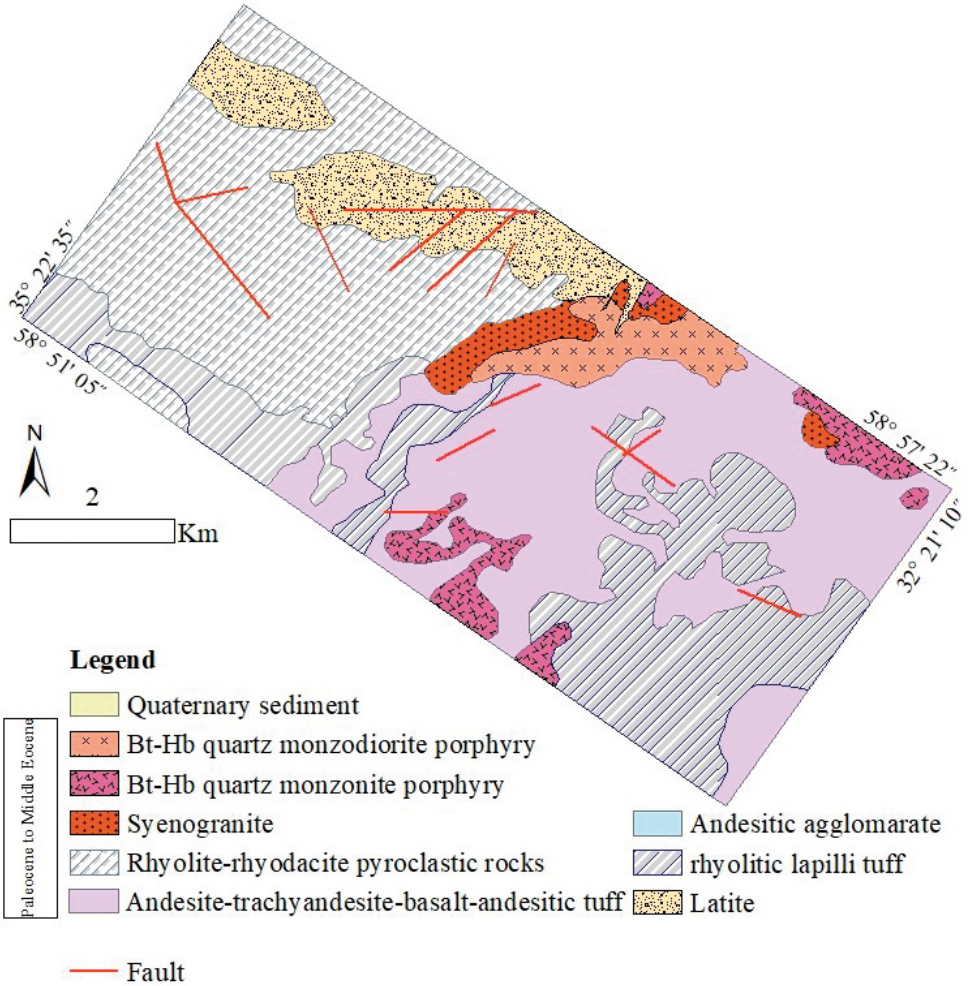

Figure 6. Simplified geology map of Kuh-e- Zar deposit (modified after Karimpour et al., 2017) NE Iran. The prevailing stratigraphic unit is composed of Cenozoic volcanic rocks (rhyolitic to andesitic in composition).

conglomerate. The veins vary in length from 350 m to >1.2 km, and from 0.5 to 5 m in thicknesses (Ashrafpour et al., 2007). Mineralogy of gangue minerals are quartz, chalcedony, calcite, adularia, illite, and minor kaolinite and barite.

The ore minerals are comprised of pyrite, arsenopyrite, minor chalcopyrite, sphalerite, galena, magnetite and hematite. Pyrite is the main sulfide mineral in the hypogene ore.

Maximum assay obtained from many trenches and drill cores for Au, Ag, As, Sb, and Hg are 83, 220, 19600, 2730, and 6.2 g/t, respectively. The vein III is the main ore system. Antimony ore vein consists intimate association of stibnite and grey to dark quartz along a fault in granite. Stibnite ore occurs as scattered patches, of 1-10 cm thick, throughout the vein (Ashrafpour et al., 2007).

Khunik hydrothermal breccia gold mineralization

The Khunik prospecting area is located 106 km south of Birjand in eastern Iran (Figure 1). The rocks in the area comprise conglomerate, volcanic and sub-volcanic units. The oldest unit exposed in the south of the study area is Palaeocene-Eocene conglomerate. There are several outcrops of granitoid sub-volcanic intrusions as dikes and stocks in the area which have intruded into the volcanic rocks (Figure 8).

Alteration, mineralization and geochemistry

Hydrothermal alteration in the Khunik area is related to some of intrusive bodies. Alteration zones exposed at the surface are propylitic, argillic and carbonate. The identified alteration in boreholes are quartz-sericite-pyrite ± tourmaline and carbonatization. Alteration shows

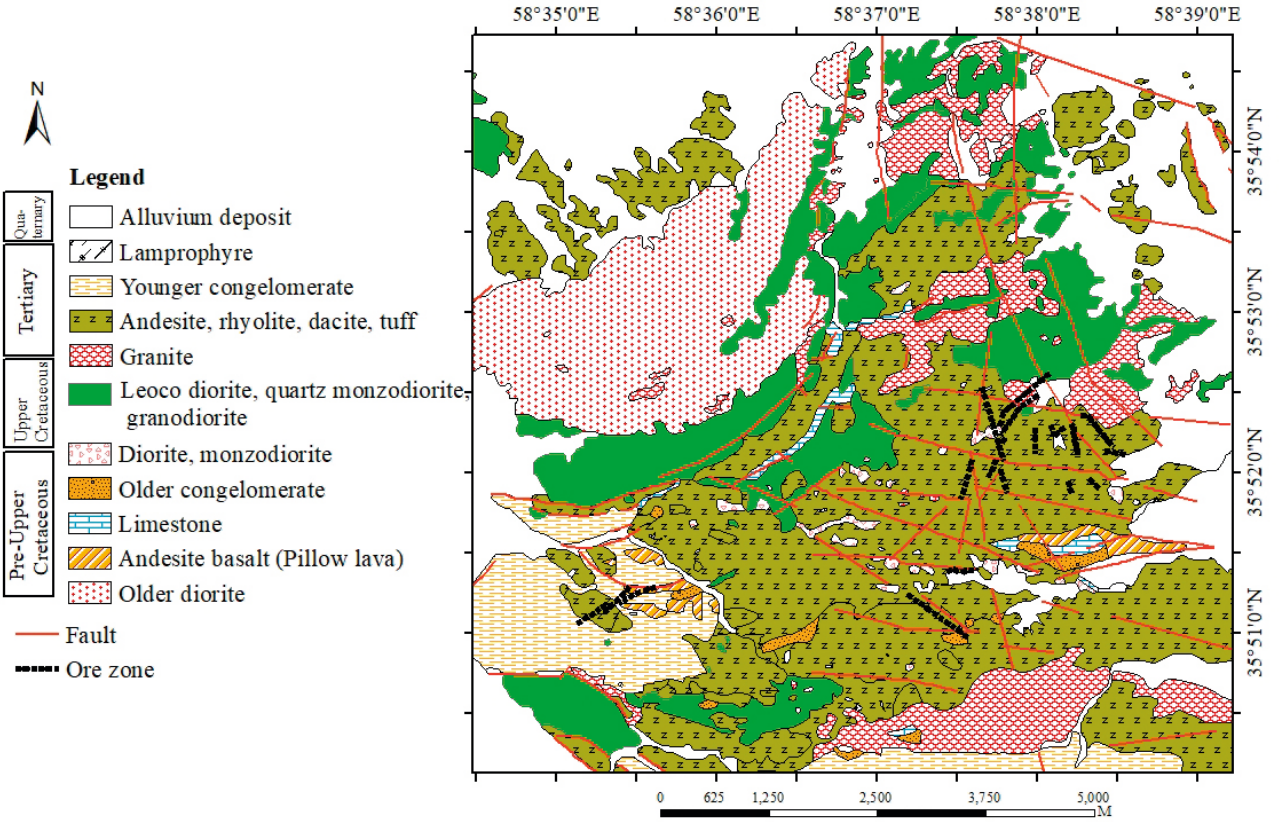

Figure 7. Geology map of the Arghash deposit (modified after Alaminia et al., 2013).

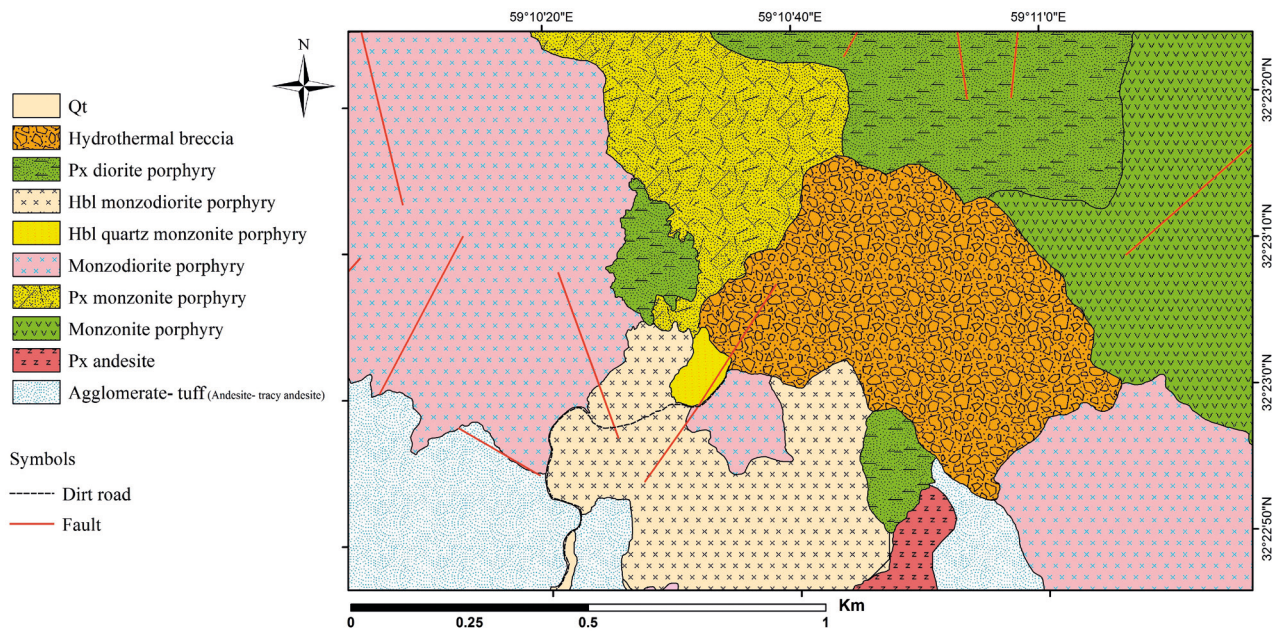

Figure 8. Geology map of the Khunik area (Samiee, 2015).

zoning such that quartz-sericite-pyrite lies at the centre and propylitic and argillic lies in the margins (Samiee, 2015).

Mineralization crops out in the central portion of the area as disseminated, veinlet, stock-work, and hydrothermal breccia. Hydrothermal breccia is the most important type of the mineralization in this prospecting area (Figure 9A, B and C).

Metallic minerals present are dominantly pyrite, and only in trace amounts, include chalcopyrite, tetrahedrite and galena. Most probably, intrusion of monzodiorite porphyry to diorite porphyry into the active hydrothermal system in the Khunik area would have caused phreatomagmatic and phreatic eruption and produced breccia zone in the area.

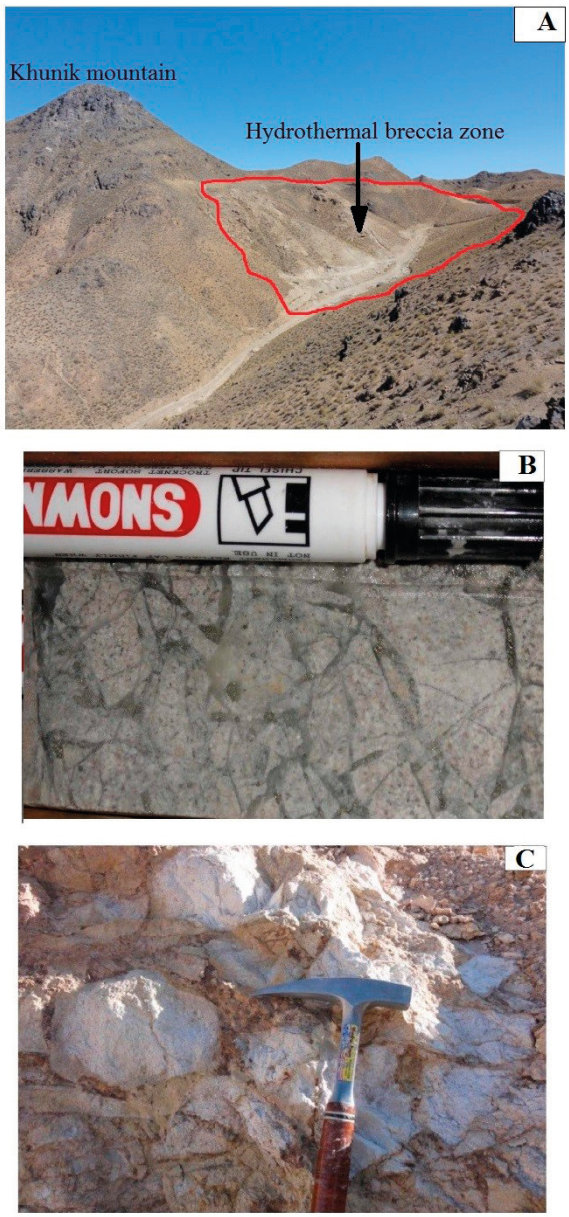

Figure 9. A) View of Hydrothermal breccia zone in the Khunik area, B) Hydrothermal breccia at depth (153.7 m). C) Outcrop of hydrothermal breccia at surface of the Khunik area.

Fluid inclusion studies was conducted on four stages of mineralization and the results are outlined as follows:

- The first stage of the mineralization involves disseminated mineralization in quartz-sericite- pyrite alteration with average temperatures as 302.5 °C and 3.04 wt% NaCl eq.
- The second stage crops out as veinlet to stock-work in quartz-sericite-pyrite alteration. The result of fluid inclusion studies in anhydrite-pyrite veinlet and quartz-pyrite veinlet show average temperature as 140.6 °C, 176 and 3.04 °C, and salinity as 3.04, 4.9 and 4.24 wt% NaCl eq. respectively.
- The third stage of mineralization contains cement of hydrothermal breccia. The fluid inclusions have average homogenization temperature of ~329 °C, and salinities of 6.32 wt% NaCl eq.
- The fourth stage of mineralization consists of carbonate-quartz-galena vein with T_h=329 °C and salinity=4.88 wt% NaCl eq.

Based on the lithogeochemical data, concentration of the elements are as follows: Au: 2-4600 ppb, Ag: 40-980 ppb, Sb: 6.9-133.5 ppm, As: 0.5-158 ppm, Hg: 0.2-4.95 ppm, Cu: 21-601 ppm, Pb: 4-1485 ppm, Zn: 18-1095 ppm. Geochemical data in the drill cores indicated anomalies with different variations in gold concentration.

Chah Shaljami high-sulfidation epithermal gold deposit

Chah Shaljami exploration area is located 190 km south of Birjand (Figure 1). It is a broadly-circular alteration zone hosted by Eocene andesitic volcanic and pyroclastic rocks that have been intruded by late Oligocen sub-volcanics as stocks and dikes. (Figure 10). These stocks and dikes are composed of quartz monzodioritic and hornblende granodiorite. Granodiorite rocks are distributed as small stocks of Oligocene age (Arjmandzadeh et al., 2011). Quartz monzonite stocks are the most extensive intrusive bodies in this area.

Alteration, mineralization and geochemistry

The alteration shows zoning, and includes propylitic, sericitic, chlorite-sericitic, montmorillonite, quartz-dickite, quartz-alunite and vuggy quartz from centre toward margin of mineralization.

The mineralization is as vein, veinlet, stockwork and disseminated, and includes pyrite, magnetite, arsenopyrite, molybdenite, chalcopyrite, sphalerite, galena and enargite. Intense supergene alteration has affected sulfide minerals

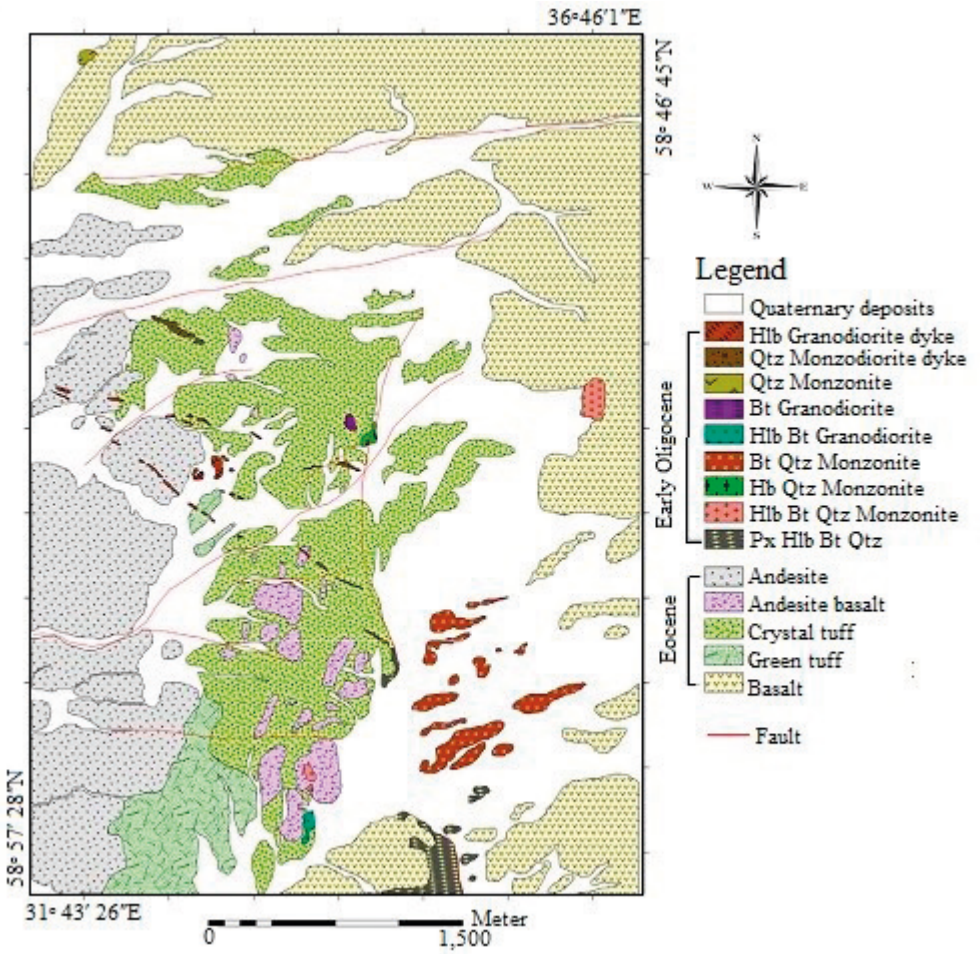

Figure 10. Geology map of the Chah Shaljami area (Arjmandzadeh et al., 2011).

at the surface and the extensive presence of malachite and chrysocolla (Arjmandzadeh et al., 2011).

Geochemical analysis of ore elements on silicification alteration and vuggy quartz shows gold anomalies of up to 0.3 ppm. In addition, there are anomalies of Sb, As, Bi, Zn, Pb, Mo in this deposit. Homogenization temperature varies between 200-570 ºC and salinity between 5 to 55 wt% NaCl eq. Temperature- salinity of fluid inclusion decreases toward the vuggy quartz alteration which indicates increase of the role of meteoric fluids (Arjmandzadeh et al., 2011).

RIRGS (Reduced Intrusion-Related Gold Systems)

Tarik-Darreh gold-antimony deposit

Tarik-Darreh prospect area is located 30 km to the north of Torbat-e-Jam in Khorasan Razavi Province, north-eastern Iran (Figure 1). The study area is mainly comprised of Jurassic slightly metamorphosed sedimentary rocks including shale, siltstone, and sandstone (Figure 11). These rocks have been intruded by plutonic rocks such as gabbro norite, diorite, quartz diorite and rhyodacite (Ghavi et al., 2018).

Alteration, Mineralization and geochemistry

Alteration is not pervasive in the study area, and is mostly indicative of clay (montmorillonite and illite), quartz-sericite, Fe-oxide, and chloritic alterations. The alteration is more intense at the contact of the quartz-diorite and gabbrodiorite and their country rocks. These zones are sometimes accompanied by arsenopyrite-bearing quartz-silica veins. The largest extension of the alteration is observed in the plutonic rocks and is often accompanied by brecciation (Shabani et al., 2010).

The mineralization in the Tarik-Darreh deposit bears a general E-W trend and is mainly of the vein-type in association with the contact of the quartz-diorite intrusive rocks with shale and siltstone units (Ghavi et al., 2018).

The silica veins are 1 to several centimetres long with

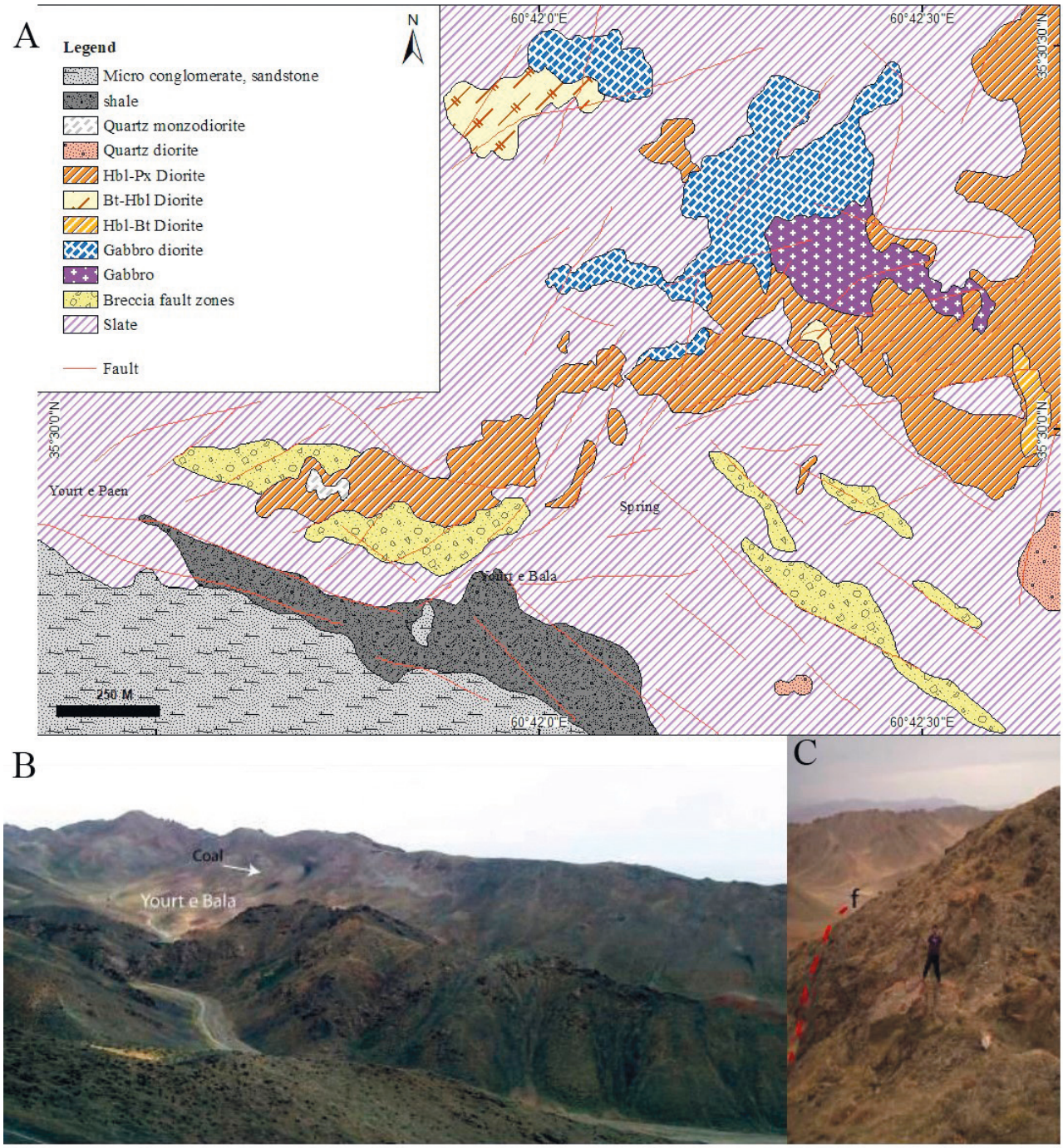

Figure 11. A) Simplified geology map of the Tarik Darreh deposit (modified after Ghavi et al., 2020); B) Outcrops of different rock units in the Tarik Darreh area, looking east; C: Fault breccias in south part of the Tarik Darreh area, looking south.

arsenopyrite concentration which reach occasionally up to 90%. Ore microscopy investigations indicate arsenopyrite, pyrite, and chalcopyrite as the main ore minerals. Native gold was observed only in one section as inclusions in arsenopyrite. The presence of arsenopyrite, chalcopyrite and pyrite-bearing silica veins, together with gold in relation to these alterations indicate the significance of this phase of intrusion and its fertility for mineralization (Shabani et al., 2010; Ghavi et al., 2018).

According to Shabani et al., 2010, gold is the

most promising element (0.45 to 12.9 ppm). Silver, arsenic, copper, bismuth, and tellurium show also high concentrations, 15.7 ppm, 70600 ppm, 1540 ppm, 25600 ppm, and 216 ppm, respectively.

Hired gold-Tin prospecting deposit

Hired deposit is located 140 km southwest of Birjand in the Khorasan Jonubi province (Figure 1). Exposed rocks at Hired gold-tin prospecting area are mainly Mesozoic and Paleocene sedimentary and Eocene volcanic rocks (Figure 15). Oligo-Miocene granitoids have intruded into the Eocene and older rock units. Based on magnetic susceptibility values, granitoids are of two types: 1) ilmenite series in the central and western parts of the area and comprise quartz monzonite and granite porphyry. The ilmenite-series granitoids are the source rocks of mineralization. 2) magnetite-series, including gabbro, norite-gabbro and diorite in the eastern part of area (Figure 12), (Karimpour et al., 2006).

Alteration, mineralization and geochemistry

Ilmenite-series granitoids have played a major role in the mineralization at this area and led to extensive alterations. The most important alterations related to gold mineralization are tourmaline zones, quartz-tourmaline-

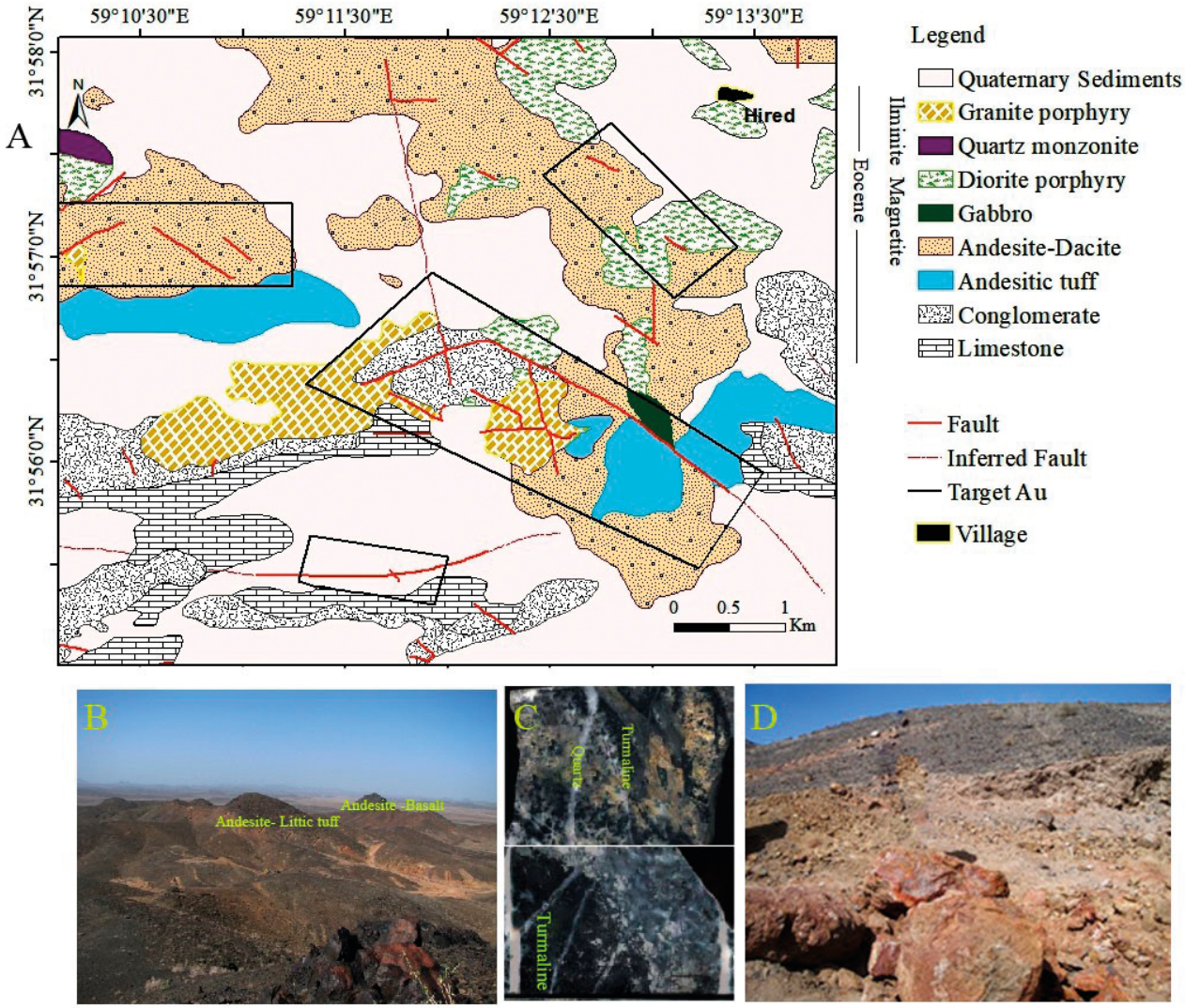

Figure 12. A) Geology map of the Hired deposit (modified after Askari et al., 2015), B) Field photograph from the Hired prospect area, looking northwest, C) Stockwork mineralization associated with tourmalinization, D) field photograph of mineralization, looking east.

sericite and silicic-carbonate. Propylitic alteration is widespread, whilst, is not related to gold mineralization. This type of alteration is formed in magnetite-series granitoids and around volcanic rocks and comprise chlorite, epidote, carbonate and quartz. Skarn has also formed as a result of contact metasomatic processes in conglomerate, related to reduced intrusive rocks (Karimpour et al., 2006; Askari et al., 2015).

The most important and diffuse mineralization is located in the central part of the Hired area, and is around the ilmenite-series granitoid (Karimpour et al., 2007). Stockwork and disseminated are dominant type of mineralization occur within these intrusions and in the eastern part of the Hired area. In addition, massive, replacement, skarn and vein type are of other styles of mineralization in the Hired deposit. There are quartz-sulphide veins within the volcanic rocks in northwestern and conglomerate-limestone in the south and east of the intrusions. ore minerals in the Hired deposit are arsenopyrite, pyrite, pyrrhotite, chalcopyrite, sphalerite and galena. Tourmaline, quartz, calcite, chlorite and sericite are the main gangue minerals. Most of the arsenopyrite, pyrrhotite, and chalcopyrite minerals occur as disseminated and stockwork within and adjacent to the granite porphyry stock at the first stage of mineralization (300-420 °C). In contrast, the concentration of pyrite increases within distal veins (190-290 °C (Karimpour et al., 2021). Gold is associated with sulfide-silica-tourmaline veins (Karimpour et al., 2006, 2021).

Gold grade in the Hired deposit varies from 5 ppm within, and in the vicinity of the ilmenite-series granitoids (especially granite porphyry), to 57 ppb Au at distal zones. The highest concentration of Ag (120 ppm), Zn (2053 ppm) and Cu (3500 ppm) in addition to a significant concentration of Sn (580 ppm) is also related to this part of the mineralization (Askari et al., 2015). Generally, the highest concentrations of Au, Ag, Cu, Pb, Zn, As and Sb are located in the east of the exploration area along with stockwork mineralization, which is the main type of mineralization (Karimpour et al., 2006).

Mesozonal orogenic type

In the EI, lies only one orogenic-type deposit as follow:

Torghabeh Mesozonal Orogenic (pyrrhotite, pyrite, arsenopyrite) Gold Deposit

Torghabeh Gold Deposit (TGD) is located 8 km west of Mashhad (Figure 1). The Torghabeh area is part of a collisional zone formed during the Late Paleozoic-Early Triassic times due to the collision of Iran and Turan plates. Oldest exposed rocks are meta-ophiolite and meta-flysch (Paleo-Tethys remnants). Dehnow-Vakilabad-Torghabeh tonalite granodiorite (Upper Triassic, Karimpour et al., 2010) has intruded low-grade regional metamorphosed rocks of Late Paleozoic (Figure 13). Different types of schists have formed around the contact (Karimpour et al., 2006).

Alteration, mineralization and geochemistry

Hydrothermal fluids in the shear zone (breccia) have caused alteration in metamorphic and igneous rocks in this area. The intensity of alteration decrease with distance from this zone. Some four types of alteration related to mineralization were determined in this region, entailing silicified, propylitic, argillic and sericitic alteration. Of these, silicified alteration is dominant and the others are of inconsiderable spread.

Mineralization is found within NW-SE-trending shear zones. The shear zones crosscut all of the exposed rocks, so that mineralization is younger than the host rocks. The width of mineralization is between 0.4 to 2.5 m and its length is ~750-800 m. Mineralization in the shear zones has occurred as open space filling and stockworks. Parageneses from depth to the surface are, 1) arsenopyrite-pyrrhotite-gold, (2) pyrite-arsenopyrite-gold, and (3) pyrite-gold-galena. Gold is mainly associated with pyrite and arsenopyrite. The elemental content of Ag, Bi, Cu,

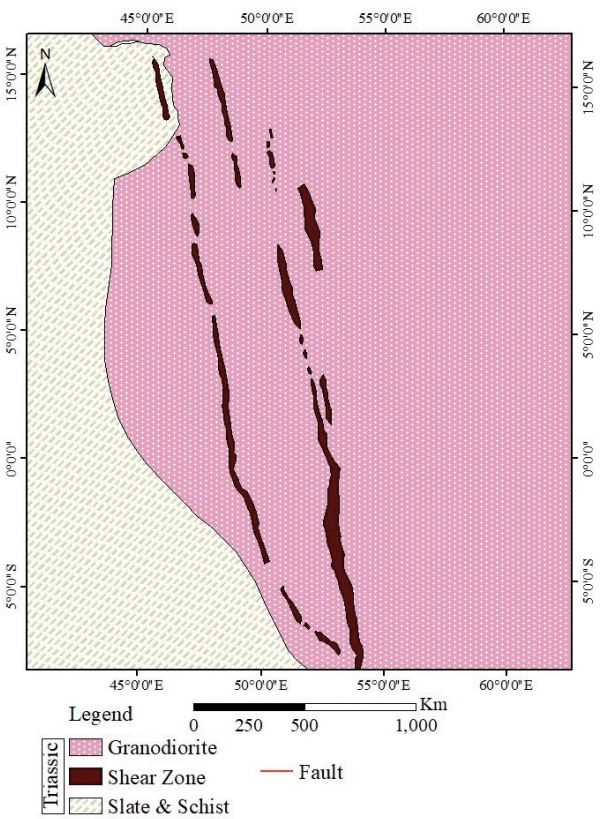

Figure 13. Geology map of the TGD (modified after Karimpour et al., 2006).

Sb, Sn, Pb, Zn and W is low. Gold grade varies between 0.5 to 56 ppm and is <5 ppm on average. The ore-bearing solution has been in reducing stage, low in S and T= 420 °C, pH=7, Log fO_2<-40, Log fS_2<-14 (Karimpour et al., 2006).

GEOCHEMISTRY OF HOST ROCKS OF GOLD MINERALIZATION IN THE EI

Geochemical data were gleaned from a variety of literature (e.g., from Mohmmadi, (2006) and Karimpour et al., (2005) for the Qale-Zari deposit; Amraie and Niroumand (2014) for the Koodakan deposit; Mazloumi et al. (2008) and Karimpour et al. (2017) NE Iran. The prevailing stratigraphic unit is composed of Cenozoic volcanic rocks (rhyolitic to andesitic in composition for the Kuh-e-Zar deposit; Alaminia et al. (2013) for the Arghash deposit, Samiee (2015) for the Khunik deposit; Arjmandzadeh et al. (2011) for the Chah Shaljami deposit; Ghavi et al. (2020) for the Tarik Darreh deposit; Karimpour et al. (2007) for the Hired deposit; and Karimpour et al. (2010) for the Torghabeh deposit. These data are representative of the compositional characteristics of host rocks for gold deposits in the EI; notwithstanding appropriate geochemical data are not available for all parts of this area especially for the Arghash, Tarik Darreh and Koodakan deposits.

The majority samples of Qale-Zari deposits were plotted in the fields of monzonite, gabbro diorite, diorite, and monzodiorite of the TAS diagram (Figure 14). Magnetic susceptibility for these units have high values (104× 10^{-5} SI to 4678×10^{-5} SI) (Mohammadi, 2006) which is indicative of the magnetite series of Ishihara (1981). These rocks are shoshonitic to calc-alkaline high-K series (Figure 15).

The major rock types in the intrusive rocks spatially close to mineralization in the Kuh-e-Zar deposit are diorite, quartz monzonite, monzonite and granodiorite (Figure 14), and include calc-alkaline high-K to shoshonitic (Figure 15), and I-type. Karimpour et al. (2017) NE Iran. The prevailing stratigraphic unit is composed of Cenozoic volcanic rocks (rhyolitic to andesitic in composition suggest the zircon U-Pb ages of ca. 40.7-41.2 Ma for these intrusive rocks. Magnetic susceptibility of these units are >50×10^{-5} SI and belong to magnetic series (Mazloumi and Rasa, 2009).

The sub-volcanic rocks related to mineralization in the Khunik area are diorite, monzonite and quartz-monzonite (Figure 14). The age of this units based on U-Pb zircon dating is 38±1 Ma. (Samiee et al., 2016). Measurement of magnetic susceptibility for the rock types provides high values (236×10^{-5} SI to 4800×10^{-5} SI). These rocks plot as calc-alkaline high-K to shoshonitic series (Figure 15).

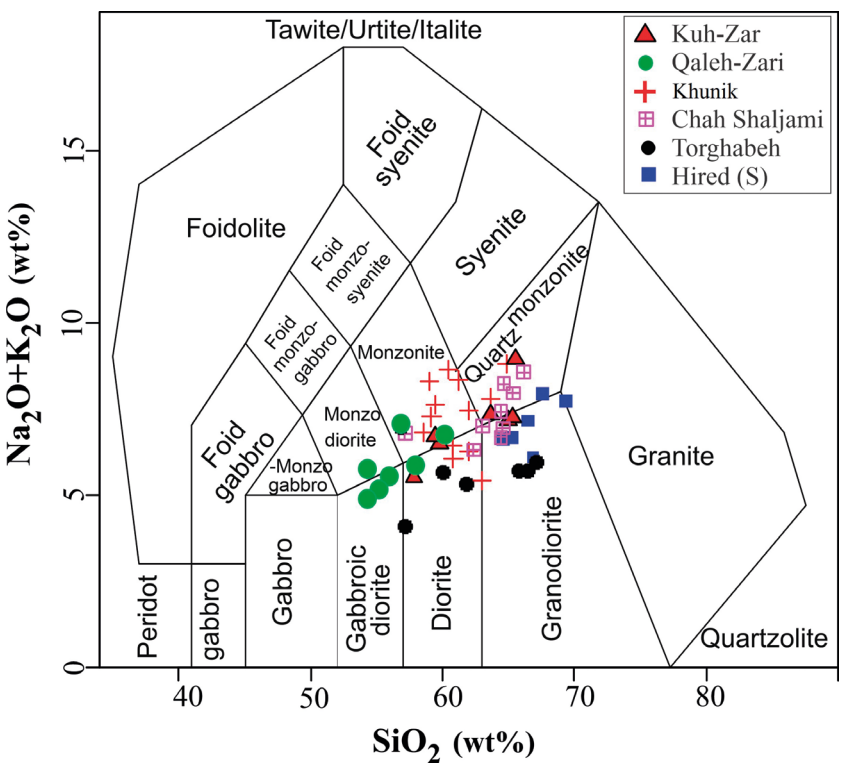

Figure 14. Total alkali-silica diagram (Middlemost, 1994), showing samples from the intrusive host rocks of gold mineralization in the EI (See the section 4, for data references).

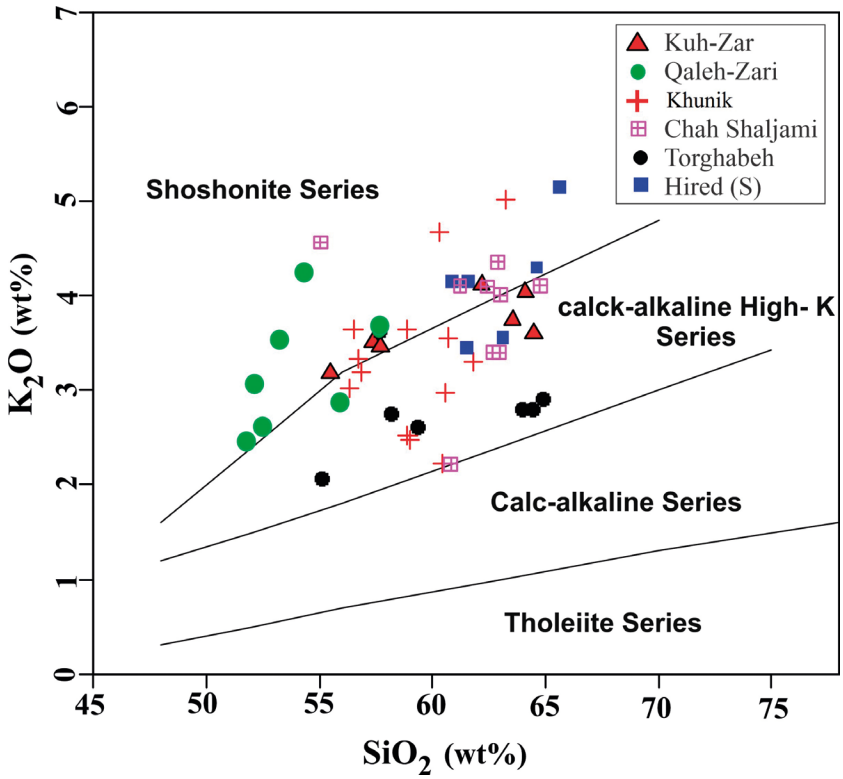

Figure 15. K_2O vs SiO_2 diagram (Peccerillo and Taylor, 1976) of intrusive of host rocks of gold mineralization in the EI (See the section 4, for data references).

Intrusions related to mineralization in Chah Shaljami are mostly quartzmonzonit, granodiorite to diorite (Figure 14). Arjmandzadeh et al. (2011) determined the Rb-Sr age of 33.5±1 Ma. for these rock units. Magnetic susceptibility varies from 2300×10-5 to $<10\times10^{-5}$ (SI units). These rocks have features typical of high-K calc-alkaline to shoshonitic (Figure 15).

In the Hired deposit, there are two type of granitoids as I- and S-type (Karimpour et al., 2007). S-type granitoids are related to mineralization, and are compositionally granodiorite and quartz monzonite (Figure15). They are shoshonitic to calc-alkaline high-K series (Figure 16). Magnetic susceptibility of S-type granitoids is $<55\times10^{-5}$ SI (Karimpour et al., 2007). Zircon U-Pb dating indicates the age of 37.8 Ma for ilmenite-series granite in Hired (Karimpour et al., 2021)

The granitoids in the TGD are granodiorite and diorite in composition (Figure 14) and are calc-alkaline high-K (Figure 18). Zircon U-Pb dating indicates that the age of 215±4 Ma for this granitoids (Karimpour et al., 2010). They have magnetic susceptibilities between 5×10^{-5} and 20×10^{-5} (SI units) and therefore are classified as belonging to the ilmenite series of reduced-type granitoids. (Karimpour et al., 2010).

Most of the intrusive rocks of Qale-Zari gold mineralization have quite similar REE characteristics (Figure 16). Patterns for rocks are essentially parallel and rocks are significantly light rare earth elements (LREE) enriched with well-developed negative Eu anomalies (Figure 16) with $(La/Yb)_N$ values of 12.2-16. In Sr/Yb vs Y plot (Figure 17), intrusive rocks of Qale-Zari plot in normal island arc calc-alkaline domain and have oxidize character (Figure 18). The chondrite-normalized (Pearce, 1983) rare earth element samples characterized by relatively flat heavy rare earth elements (HREE) and there is a significant enrichment in LREE (Figure 19).

Intrusive rocks that host mineralization in the Kuh-e-Zar deposit in chondrite-normalized REE patterns (Figure 16), are characterized by LREE moderate enrichment ($(La/Yb)_N$=7-8.72), by HREE depletion and mostly by negative Eu anomalies (0.63-1.03), and all samples plot in normal island arc calc-alkaline (Figure 17), and intrusive rocks plot in oxidizing realm (Figure 18). In the context of MORB patterns, trace element abundances in the Kuh-e-Zar deposit (Figure 19) show enrichment in large-ion-lithophile elements (LILE), such as K, Rb, Ba and Th, and the most characteristic high-field strength elements (HFSE) - e.g. Nb, Zr, Y, Ti and HREE - possess lower normalized values compared to LILE; in particular, there are steep negative anomalies in Nb (Figure 19). These

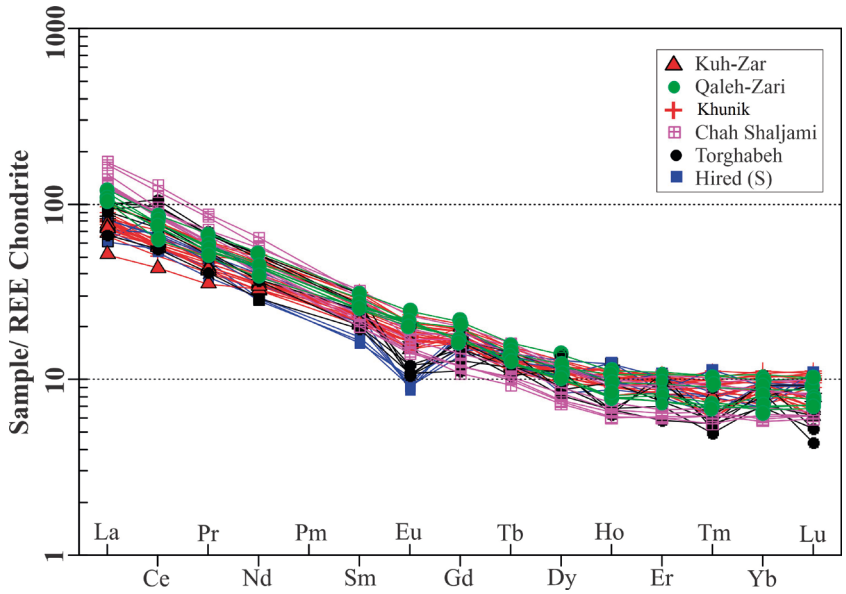

Figure 16. Chondrite-normalized REE diagrams for samples of the intrusive host rocks of gold mineralization in the EI (Boynton, 1984, See the section 4, for data references).

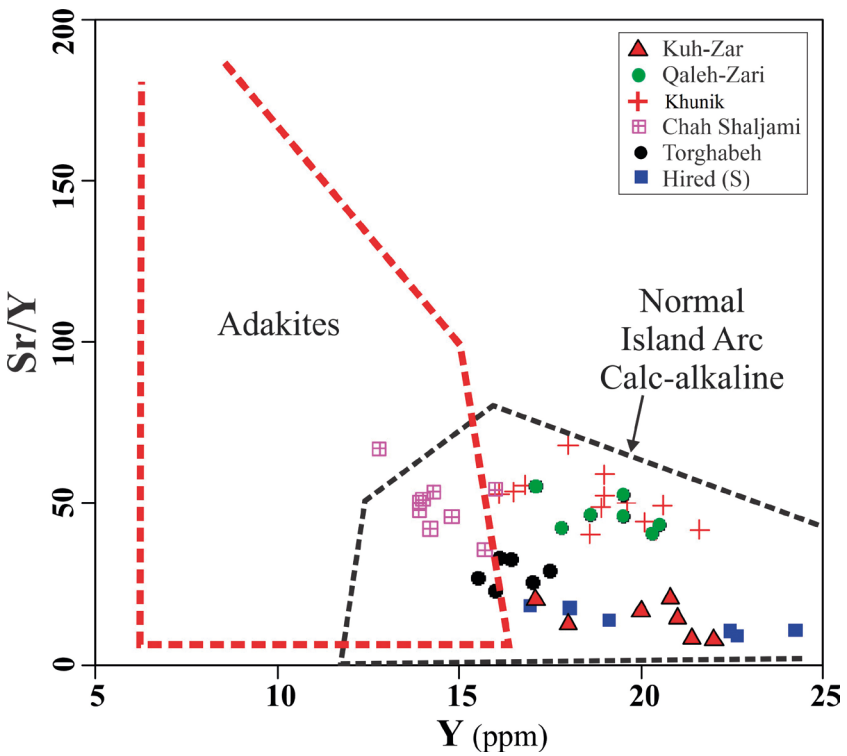

Figure 17. Sr/Yb vs Y plot samples of the intrusive host rocks of gold mineralization in the EI (Defant and Drummond, 1990, See the section 4, for data references).

features are typical of the subduction-related magmas, namely in the calc-alkaline volcanic arcs of continental active margins.

According to chondrite normalized REE diagram (Figure 16), all the sub-volcanic samples in the Khunik deposit show similar patterns, and are enriched in LREE.

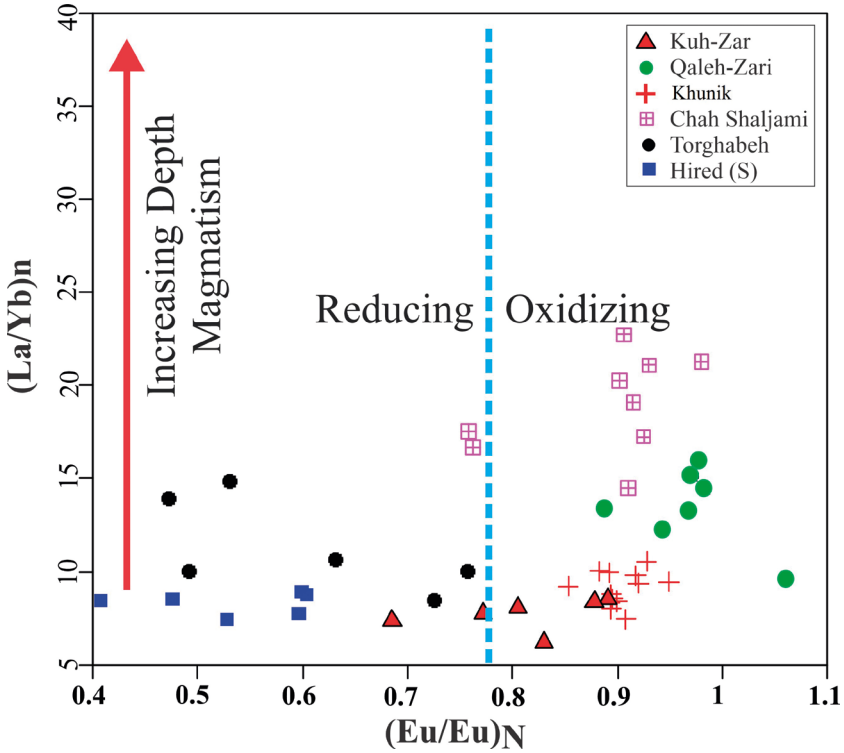

Figure 18. Chondrite normalized La/Yb vs (Eu/Eu) N diagram, demonstrating compositional characteristics of host rocks in gold deposits in the EI (See the section 4, for data references). Dividing line between reducing and oxidizing magma, and increasing trend of depth of magmatism by Karimpour and Sadeghi (2019).

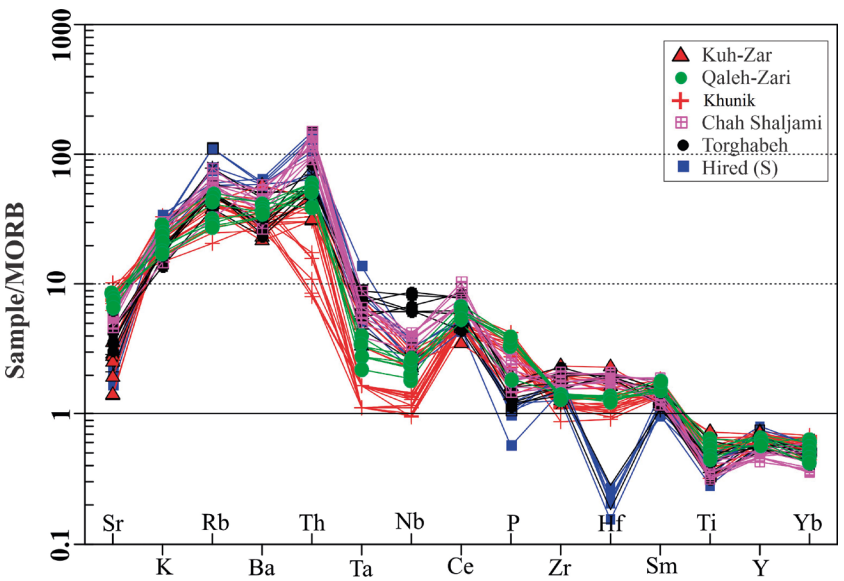

Figure 19. MORB (Pearce, 1983) trace element diagrams for samples of the intrusive host rocks of gold mineralization in the EI (See the section 4, for data references).

The La_N/Yb_N of sub-volcanic rocks range between 7.45- and 10.54. On the diagram of $(La/Yb)_N$ vs Yb_N (Li et al., 2008) and Sr/Y vs Y (Defant and Drummond, 1990) (Figure 17), all samples are plotted in the realm of classic island arc. The Khunik samples have no Eu anomalies (Eu/Eu*=0.85-0.95) and are oxidized (Figure 18).

In the MORB trace element diagrams for Khunik intrusive rocks (Figure 19), all samples are enriched in highly incompatible elements such as LREE and LILE such as Sr, K, Rb, and Ba, however, depleted in HFSE, with prominent negative anomalies of Ta-Nb and Ti. This high LIL/HFS pattern is now recognized as a distinctive feature of subduction zone magmas (Gill, 1981; Ma et al., 2014; Pearce, 1983; Rollinson, 1993; Wilson, 1989; Winter, 2001).

REE patterns in chondrite-normalized plots for intrusive host rocks in the Chah Shaljami deposit display high degrees of REE fractionation (Figure 16), with strong LREE enrichment (22.7 P La_N/Yb_N P 14.4). Their strong resemblance to each other suggests that the studied intrusives are genetically related and most likely derived from the same initial melt. Most of the studied rocks have Eu/Eu* ratios from 0.90 to 0.98. Sr/Y ratio of the Chah Shaljami intrusives is 19.7-67, overlapping the values reported for adakites (Kepezhinskas et al., 1997; Castillo et al., 1999) (Figure 17). In Figure 21, these units are plotted in oxidizing part that confirm magnetic susceptibility values and I-type granitoids character.

The MORB trace element diagrams (Figure 19) display strong enrichment in LILE, such as Rb, Ba and K. The most characteristic HFSE - e.g. Nb, Ta, Y, Ti and HREE - have, compared to LILE, clearly lower normalized values; Nb, Ti, in particular, define deep negative anomalies. These features are typical of the subduction-related magmas, namely in the calc-alkaline volcanic arcs of continental active margins.

REE patterns in chondrite-normalized plots for intrusive rocks in Hired display low LREE/HREE fractionation with an average $(La/Yb)_N$ of 7.5-7.8 and negative Eu anomalies for S-type (Figure 16).

They plot in island arc realm (Figure 17). The S-type granitoid in Hired is reduced (Figure 18).

In the MORB diagram, samples of S-type granitoids are enriched in LILE, such as Rb, Th, K, whilst have negative anomalies in Ba, P and Ti and especially Hf (Figure 19).

P depletion in Hired area intrusions may be considered due to apatite fractionation (Gust et al., 1997; Woodhead et al., 1993). Low concentration of Hf in Hired intrusions are indicator for more differentiated and low partial melting of magma (Linnen, et al., 2014).

REE analyses (normalized with respect to chondrites (Boynton, 1984) indicates that the plutonic rocks in the Torghabeh deposit exhibit similar chondrite-normalized REE patterns which are characterized by moderate LREE enrichment and medium HREE enrichment (Figure 15). They have total rare earth contents of 100-180 ppm and La_N/ Yb_N=6.33-11.38 and place in normal island arc calc-alkaline position in Figure 20. The ratios of Eu/Eu* vary from 0.74 to 1.1, therefore, these rocks have small negative or no Eu anomalies (Eu/Eu*<1.0). These rocks are plotted in reduce-type granitoid realm (Figure 19) that is confirmed by magnetic susceptibility values.

Well-defined negative anomalies are observed in the MORB trace element diagram (Figure 22) of representative samples of the diorite and granodiorite for P, Ti, Sr, and Nb. Fractionation or presence of some minerals in the restites explains the negative anomalies, for example, apatite (P) and ilmenite and/or titanite (Ti). The LFSE elements of Ba and Rb show positive anomalies (Karimpour et al., 2010).

In order to determine the tectonic setting of the intrusive host rocks from the gold mineralization in the EI, the tectonic discrimination diagrams of Pearce et al., (1984) are applied (Figure 20). These rocks plot almost on the realms of the volcanic arc granites (VAG), except for some samples of S-type granitoids in the Hired deposit that place in the boundary with syn-collision granitoids realm.

Sr and Nd isotopic composition

Some radiogenic isotopic data have been produced for some of the intrusive rocks in the gold mineralization in the EI (Tables 1 and 2).

The two monzodiorite and monzogabbro samples of the Qale-Zari deposit have initial $^{87}Sr/^{86}Sr$ ratios of 0.705037-0.705330 (Table 1), initial $^{143}Nd/^{144}Nd$ ratios of 0.512626 with $\varepsilon Nd_{(t)}$ of 0.75 (Table 2, Figure 21).

The very similar initial Sr, and Nd isotope compositions in Kuh-e-Zar samples (Tables 1 and 2) suggests that most of the Kuh-e-Zar intrusions are co-genetic, deriving from the same parental magmas by magmatic differentiation processes, such as crystal fractionation (Karimpour et al., 2017 NE Iran. The prevailing stratigraphic unit is composed of Cenozoic volcanic rocks (rhyolitic to andesitic in composition). Based on the $\varepsilon Nd_{(t)}$ vs $(^{87}Sr/^{86}Sr)_{(i)}$ isotopic plot (Figure 21), the Kuh-e-Zar granitoid rocks exhibit a trend towards the upper continental crust, suggesting that crustal contamination has played a role in magma evolution (Karimpour et al., 2017 NE Iran. The prevailing stratigraphic unit is composed of Cenozoic volcanic rocks (rhyolitic to andesitic in composition).

For Chah Shaljami, initial $^{87}Sr/^{86}Sr$ and εNd values are tightly clustered in the ranges from 0.70470 to 0.70506 (Table 1) and from +1.9 and +2.7 (Table 2), respectively. In the εNd vs $(^{87}Sr/^{86}Sr)_{(i)}$ diagram (Figure 21), this cluster plots to the right of the so-called mantle array and overlaps the realm of island-arc basalts. The very similar initial Sr and Nd isotope compositions in the five samples cluster suggest that most of the Chah Shaljami intrusives are co-genetic, deriving from the same parental magmas by magmatic differentiations processes, such as crystal fractionation. Taking into account the IAB like isotope compositions of the studied rocks, the parental magmas

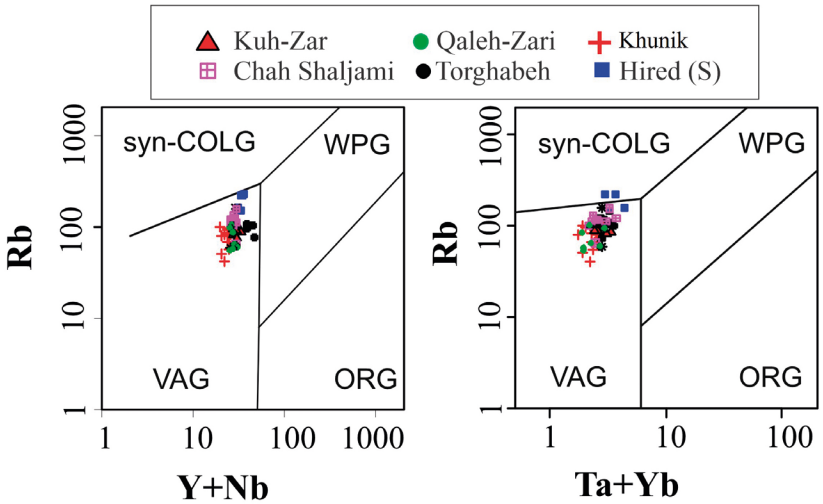

Figure 20. Plot of sub-volcanic host rocks of gold mineralization in the EI on tectono-magmatic diagram (Pearce et al., 1984), (See the section 4, for data references). VAG=volcanic arc granite, syn-COLG=syn-collision granite, WPG=within plate granite, ORG= orogenic granite.

Table 2. Rb-Sr whole rock data from the investigated areas.

Name	Rock Type	Age (Ma)	Rb	Sr	$^{87}Rb/^{86}Sr$	$^{87}Sr/^{86}Sr$ (m)	$^{87}Sr/^{86}Sr(i)$	References
Qale-Zari	Monzodiorite-monzogabbro	41 to 38	102	827	0.3570	0.705234	0.705037	Karimpour et al. (2017)
			64	1268	0.1460	0.705411	0.705330	
Kuh-e- Zar	Monzodiorite porphyry	41.2	81.9	348	0.6322	0.706719	0.706355	Ghavi (2018)
	monzonite porphyry	40.9	86	166	1.4753	0.706828	0.705963	Karimpour et al. (2017)
	Syenogranite		166	57	0.0850	0.706457	0.706408	
Chah Shaljami	Granodiorite	-	88.9	171	0.7384-1.5242	0.705913-0.706910	0.705488-0.706033	Arjmandzadeh et al. (2011)
	Monzonite	33.5	118.8	668.1	0.0150	0.704944	0.704700	
	Granodiorite	-	222.5	598.2	0.0300	0.706007	0.705090	
Khunik	Diorite porphyry	38.4	81	1019	0.2300	0.704774	0.704650	Samiee et al. (2016)
	Granodiorite porphyry	31.3	52.4	689	0.2200	0.704789	0.704692	
Hired	Granite (Il)	37.7	173.4	215	2.3287	0.707499	0.706270	Karimpour et al. (2021)
Arghash	Granite	55.4	78	123	1.8387	0.705579	0.704142	Alaminia et al. (2013)

Il: Ilmenite

might have been formed through partial melting in a supra-subduction mantle wedge.

In the Khunik area, all the samples of sub-volcanic rocks have similar radiogenic and relatively homogeneous Sr-Nd isotopic values, $(^{87}Sr/^{86}Sr)_{(i)}$ goes from 0.704196 to 0.704772 (Table 1) and $\varepsilon Nd_{(i)}$ varies between +1.3 and +3.3 (Table 2, Figure 21) (Samiee et al., 2016). According to Chappell and White, (1974), values of $(^{87}Sr/^{86}Sr)_{(i)}$ below 0.708 are characteristic of I-type granitoids. Therefore, the obtained values provide further evidence

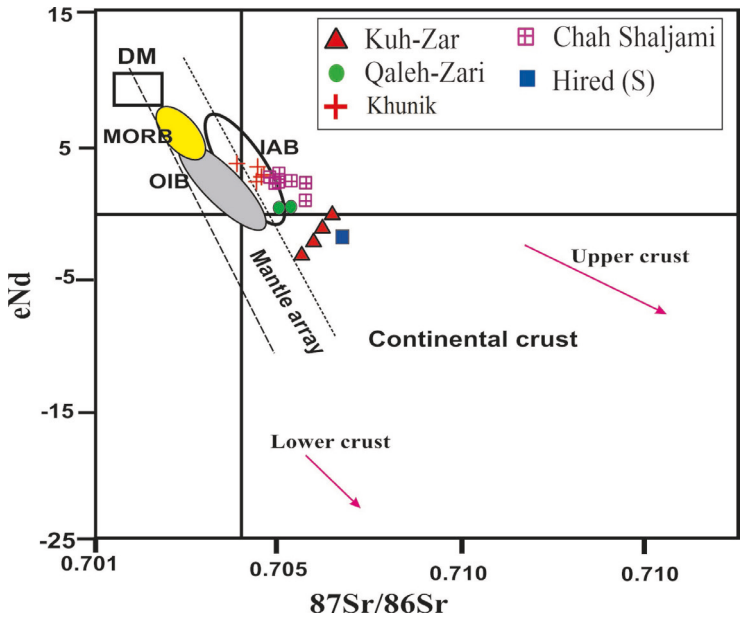

Figure 21. $\varepsilon Nd_{(i)}$ vs $(^{87}Sr/^{86}Sr)_{(i)}$ diagram for the Kuh-e-Zar (Karimpour et al., 2017 NE Iran. The prevailing stratigraphic unit is composed of Cenozoic volcanic rocks (rhyolitic to andesitic in composition), Khunik (Samiee et al., 2016) and Chah Shaljami (Arjmandzadeh et al., 2011). Reference data sources: upper continental crust (Taylor and McLennan, 1985); lower continental crust (Rollinson, 1993; Rudnick, 1995) with those of MORB (Rollinson, 1993; Sun and McDonough, 1989involving no significant change in the environment of formation for MORBs and OIBs. In detail, minor differences in element ratios correlate with the isotopic characteristics of different types of OIB components (HIMU, EM, MORB), DM (McCulloch and Bennett, 1994), OIB (Vervoort et al., 1999), IAB (Arjmandzadeh and Santos, 2014), and mantle array (Wilson, 1989; Gill, 1981; McCulloch et al., 1994).

in favour of the I-type nature of the studied granitoids. In addition, the obtained Sr and Nd isotope ratios and their limited variations suggest that the parental magmas of the sub-volcanics share a subduction-related magma source (Zhang et al., 2006), these units resemble mantle-derived volcanic arc rocks and they are very similar to isotope data in Oligocene associations of K-rich granitoid rocks from Chah Shaljami (Samiee et al., 2016), which were interpreted as representing suites derived from parental magmas generated in supra-subduction mantle wedge.

The ilmenite-series mineralized granite from the Hired deposit has Sr-Nd isotope compositions of $^{87}Sr/^{86}Sri$= 0.70627 (Table 2), $^{143}Nd/^{144}Ndi$=0.512455, $\varepsilon Nd_{(t)}$=-2.60 (Table 3). In the εNd vs initial $^{87}Sr/^{86}Sr$ diagram (Figure 21), these rocks plot out of the realm of mid-ocean ridge basalts. The ilmenite-type granitic intrusive of the Hired deposit with significant difference in initial $^{87}Sr/^{86}Sr$ and εNd values, plot in the realm of continental crust (Figure 21), which shows that the continental crust has been involved in generating the acidic magma (Karimpour et al., 2021).

DISCUSSION AND CONCLUSIONS

Tertiary intrusive granitoids within the eastern Iran are mainly sub-volcanic with porphyry texture and their composition varies from granite to diorite. These are classified as belonging to the magnetite-series of I-type granitoids (exception of Hired). These rocks are meta-aluminous and those with mineralization are K-rich. In the trace-element spider diagram, all of the intrusive rocks are enriched in large ion lithophile (LILE), and are strongly depleted of high field strength elements (HFSE, Nb, P, Ti). These features are typical of subduction related magmas in the calc-alkaline volcanic arcs of continental active margins (Gill, 1981; Pearce, 1983; Walker et al., 2001; Wilson, 1989). However, significant differences in spider diagram patterns between the Hired area intrusions and other samples is related to the different sources of the magma.

Ilmenite series of Hired granitoids show negative Eu anomaly. Negative Eu anomaly could be due to several factors, including differentiation of plagioclase; lack of suspension of plagioclase differentiation due to the low content of magmatic water; low oxygen fugacity during partial melting (Frey et al., 1978; Hanson, 1980; Richards et al., 2012). Based on reduced type of granitoids of Hired, Rb-Sr isotopes and the presence of pyrrhotite, the negative Eu anomaly is due to reduced condition melting. The $(La/Yb)_n$ ratio of granitoid is being used to estimate the depth of magmatism. The $(La/Yb)_n$ ratio of Chah

Shaljami granitoids indicates that they were originated from deeper depth of subduction zone under highly oxidizing condition in comparing with other granitoids (Figure 18). Based on Eu/Eu* ratio, the oxidation state of the magma can be estimated. Qale-Zari and Chah Shaljami granitoids were formed under highly oxidizing condition (Eu/Eu*>0.85), while Hired intrusions formed in highly reducing condition (Eu/Eu*<0.7, Figure 18). The distribution of Zr, Hf, and REE yielded an estimate of the depth of the magma source, the degree of partial melting for subsequent magmatic pulses, and their evolutionary rates (Linnen et al., 2014). Low concentration of Hf with a high LREE/HREE pattern of subduction-related magmatic rocks, are indicators for more differentiated and mineralized suites (Linnen et al., 2014). Richards (2005), found that Zr, Hf, and HREE were immobile in fluid-dominated regimes and remained in a solid phase during partial melting. These features can be used to discriminate fertile from barren magmatic rocks. The Hired ilmenite series intrusions, has lower amounts Hf, with high LREE/HREE are primarily associated with Au deposit.

There are distinct differences in the radiogenic isotopic compositions, reflecting the effect of different sources in the formation of intrusions.

Through the synthesis of the salient characteristics of gold metallogeny in the EI, we arrived at the following conclusions:

1 - The gold deposits in EI can be classified into IOCG, epithermal, RIRGS and mesozonal orogenic gold deposits based on different geological features, fluid types, metal sources, and tectonic settings.

2 - The major tectonomagmatic zones that host gold mineralization in the EI are: the Lut Block, Kopeh-Dagh and Sabzevar zones. The gold deposits were formed at (1) Triassic (Tarik-Darreh and Torghabeh), (2) Eocene-Oligocene (Kuh-e-Zar, Khunik, Chah Shaljami and Arghash, and (3) Oligo-Miocene (Hired).

3 - The IOCG gold deposits distributed in Qale-Zari, Koodakan and Kuh-e-Zar are characterized by low- to moderate-homogenization temperatures (100-380 °C, predominantly 300 °C), low-to high-salinity (1-21 wt% NaCl eq., predominantly 9 wt% NaCl eq.). The formation of the IOCG ore deposits in the EI is suggested to be related to the intracontinental extension, which is possibly associated with subduction of the Lut Block.

4 - The epithermal gold deposits are distributed in the Khunik, Chah-Shaljami and Arghash with formation ranges from 33 Ma to 38 Ma. These deposits are associated with calc-alkaline intrusive complexes. The fluid inclusion data of these deposits suggest that ore deposition took place at 100 °C and 400 °C. The salinity of the ore fluids is 1-19 wt% NaCl eq.

5 - RIRGS gold deposits are distributed in the Hired and Tarik-Darreh deposits. They are associated with reduced calc-alkaline intrusive rocks.

The work presented provides an approach, through which further effective exploration for gold deposits might be undertaken.

6 - The Torghabeh deposit formed in metamorphic and igneous rocks from reduced fluid with 420 °C. Tectonically this deposit is located in collisional setting. Gold mineralization was associated with silica rich fluid.

Table 3. Sm-Nd whole rock data obtained from the investigated areas (data references the same Table 1).

Name	Sm (ppm)	Nd (ppm)	$^{147}Sm/^{144}Nd$	$^{143}Nd/^{144}Nd(m)$	$^{143}Nd/^{144}Nd(i)$	εNd
Qale-Zari	5.65	27.60	0.1240	0.512658	0.512626	0.75
	5.19	27.00	0.1160	0.512656	0.512626	0.75
	3.73	18.60	0.1178	0.512531	0.512500	-1/68
	4.11	21.20	0.1241	0.512468	0.512434	-2/93
Kuh-e- Zar	2.26	10.30	0.1179	0.512614	0.512583	-0.06
	4.28	20.61	0.1258	0.512570	0.512537	-0.96
	4.00	20.40	0.1207	0.512508	0.512476	-2.14
ChahShaljami	23.9	3.91	0.0990	0.000015	0.512735	+2.2
	34.7	5.74	0.1000	0.000011	0.512756	+2
Khunik	6.13	30.80	0.1200	0.512711	0.512681	1.8
	2.39	16.20	0.0890	0.512718	0.512700	2
Hired	4.55	23.70	0.1160	0.512483	0.512455	-2.60
Arghash	3.60	18.90	0.1152	0.512908	0.512867	5.8

ACKNOWLEDGEMENTS

We thank Dr Shirdastzadeh for her discussions and assistance for improving the manuscript and we are grateful to reviewers for their constructive comments that improved the quality of final manuscript.

REFERENCES

Alaminia Z., Karimpou M.H., Homam S.M., Finger F., 2013. Petrology, geochemistry and mineralization of Tertiary volcanic rocks associated with sub-volcanic intrusive bodies, with special reference to age dating and origin of granites from Arghash - Ghasem-Abad area, NE Iran, Journal of Economic geology 5, 1-22.

Alaminia Z., Karimpour M.H., Homam S.M., Finger F., 2013. The magmatic record in the Arghash region (northeast Iran) and tectonic implications. International Journal of Earth Sciences 102, 1603-1625.

Alavi M., 1991. Tectonic map of the Middle East, Tehran, Geological Survey of Iran, scale 1:5 000,000.

Amraie S. and Niroumand Sh., 2014. Investigation of geochemistry, mineralogy, alteration and fluid inclusion studies in Koodakan's gold-copper vein type mineralization, south Khorasan, Advance applied geology 6, 34-47.

Arjmandzadeh R., Karimpour M.H., Mazaheri S.A., Santos J.F., Medina J.M., Homam S.M., 2011. Sr-Nd isotope geochemistry and petrogenesis of the Chah Shaljami granitoids (Lut Block, Eastern Iran). Journal of Asian Earth Sciences 41, 283-296.

Arjmandzadeh R. and Santos J.F., 2014. Sr-Nd isotope geochemistry and tectono magmatic setting of the Dehsalm Cu-Mo porphyry mineralizing intrusives from Lut Block, eastern Iran. International Journal of Earth Sciences (Geologische Rundschau) 103, 123-140.

Arjmandzadeh. R., Karimpour M.H., Mazaheri S.A., Santos J.F., Medina J.M., Homam S.M., 2011. Sr-Nd isotope geochemistry and petrogenesis of the Chah Shaljami granitoids (Lut Block, Eastern Iran), Journal of Asian Earth Sciences 41, 283-296.

Ashrafpour E., Ansdell K.M., Alirezaei S., 2012. Hydrothermal fluid evolution and ore genesis in the Arghash epithermal gold prospect, northeastern Iran. Journal of Asian Earth Sciences 51, 30-44.

Ashrafpour E., Ansdell K.M., Alirezaie S., 2007. Sulfure, Carbon and oxygene isotope variation of sulfide and carbonate in Arghash gold prospect, Southwest Neishabour, Northeastern Iran, Journal of geoscience 70, 174-183.

Askari A., Karimpour M.H., Mazaheri S.A., Malekzadeh A., 2015. Interpretation of geophysical (IP/RS) in Hired gold prospecting area using geology, alteration and mineralization data, Journal of geoscience 24, 235-245.

Bache J., 1986. World Gold Deposits - A Quantitative Classification. Elsevier Science Publishing Company.

Barzegar Hassan, 2007. Geology, petrology and geochemical characteristics of alteration zones within the Seridune prospect, Kerman, Iran: Aachen, Germany, Rheinisch Westfälischen Technische Hochschule (RWTH) Aachen University, Ph.D. dissertation, 180 p.

Berberian M., 1981. Active faulting and tectonics of Iran. In: Zagros Hindukush-Himalaya Geodynamic Evolution. Geodynamics Series, 3, Gupta H.K., Delany F.M. (Eds.) American, 33-69.

Boyle R., 1979. The geochemistry of gold and its deposits. Geological survey Canada Bull. 280, 584.

Boynton W., 1984. Cosmochemistry of rare earth elements: meteorite studies. In: Henderson, P. (Ed.), Rare Earth Element Geochemistry. Elsevier, Amsterdam, 63-114.

Castillo P.R., Janney P.E., Solidum R.U., 1999. Petrology and geochemistry of Camiguin Island, southern Philippines: insights to the source of adakites and other lavas in a complex arc setting. Contributions to Mineralogy and Petrology 134, 33-51.

Cox D.P. and Singer D.A., 1986. Mineral deposit models. United States Geological Society Bull. 1693, 379 pp.

Dahooei A.H., Afzal P., Lotfi M., Jafarirad A., 2016. Identification of mineralized zones in the Zardu area, Kushk SEDEX deposit (Central Iran), based on geological and multifractal modeling. Open Geosciences 8, 143-153

Daliran F., 2008. The carbonate rock-hosted epithermal gold deposit of agdarreh Takab geothermal field, NW Iran-hydrothermal alteration and mineralization, mineralium deposit 43, 383-404.

Defant M. and Drummond M., 1990. Derivation of some modern arc magmas by melting of young subducted lithosphere. Nature 347, 662-665.

Frey F.A., Chappell B.W., Roy S.D., 1978. Fractionation of rare-earth elements in the Tuolumne Intrusive Series, Sierra Nevada batholith. California. Geol. 6, 239-242.

1:250,000 Geological quadrangle map of Iran, 1992a, No. K8: Birjand: Tehran, Geological Survey of Iran, 1 sheet.

1:250,000 Geological quadrangle map of Iran, 1992b, No. K9: Dehsalm(Chah Vak): Tehran, Geological Survey of Iran, 1 sheet.

1:5,000,000 International geological map of the Middle East, 2009, 2nd edition: Tehran, Geological Survey of Iran, 1 sheet.

Ghaderi M., Hezarkhani A., Talebi M., 2007. The use of lithogeochemical data and fluid inclusions in the study of Iju porphyry copper deposit northwest of Shahr-e-Babak, The History of Amirkabir Journal 67, 51-63.

Ghadimzadeh H., 2002. Economic geology and exploration for gold in the Safikhanlu-Noghdouz area (SE Ahar): [M. Sc. thesis]: Tehran, Iran, Faculty of Earth Science, Geological Survey of Iran, 211 pp.

Ghavi J., Karimpour M.H., Mazaheri S.A., Ghaderi M., Rahimi B., 2020. Geology, petrology, geochemistry and geochronology of Tarik Darreh plutonic rocks, northeastern Iran, Journal of economic geology of Iran 2, 203-225.

Ghavi J., Karimpour M.H., Mazaheri S.A., Pan Y., 2018. Triassic I-type granitoids from the Torbat-e-Jam area, northeastern

Iran: Petrogenesis and implications for Paleo Tethys tectonics, Journal of Asian Earth Sciences 164, 159-17.

Ghorbani M., 2002. Economic geology of Iran. Geological Survey of Iran Publication, Tehran.

Ghorbani M., 2008a. Gold in Iran, in: International Geological Congress, Oslo.

Ghorbani M., 2013. Metallogeny atlas for Iran deposits.

Gill J.B., 1981. Orogenic Andesites and Plate Tectonics, Mineral and Rocks. Springer, 16, 390 pp.

Haghipour A. and Aghanabati A., 1989. Geological map of Iran (2nd edition), Tehran, Geological Survey of Iran, scale 1:2,500,000.

Hassan Nejad A.A. and Moor F., 2002. The source of Qale-Zari copper deposits with respect to new isotopic and fluid inclusion data. Proceeding of the 6th symposium of Geological Society of Iran, Kerman, Iran, 114-117.

Hassan Nejad AA., 1993. Geology and Geochemistry of Qale-Zari Cu-Au-Ag deposit. Unpublished M.Sc thesis, University of Shiraz, Iran.

Heald P., Foley N.K., Hayba D.O., 1987. Comparative anatomy of volcanic-hosted epithermal deposits; acid-sulfate and adularia-sericite types, Economic Geology 82, 1-26.

Heidari S.M., Moosavi Makooe S.A., Mirzakhanian M., Rasoli F., Ghaderi, M., Abadi A.R., 2016. A reviwe of tectono-magmatic eolution and gold metalogeny in the inner parts of Zagros orogeny: A tectonic model for the major gold deposits, Western Iran, Eurasian mining 1, 3-20.

Jackson J. and Mckenzie D., 1984. Active tectonics of the Alpine-Himalaya belt between western Turkey and Pakistan, Geophysical Journal of the Royal Astronomical Society, 185-264.

Karimpour M., Malekzade Shafaroudi A., Mazloumi Bajestani A., Keith Schander R., Stern. Ch., Farmer L., Sadeghi M., 2017. Geochemistry, geochronology, isotope and fluid inclusion studies of the Kuh-Zar deposit, Khaf-Kashmar-Bardaskan magmatic belt, NE Iran: Evidence of gold-rich iron oxide-copper-gold deposit. Journal of geochemical exploration 183, 58-87.

Karimpour M., Malekzadeh A., Hidareian M., Askari A., 2007. Mineralization, alteration and geochemistry of Hired gold tin prospecting area, South Khorasan province. Iran. Iranian Journal of Crystallography and Mineralogy15, 67-90.

Karimpour M., Torabian A., Babakhani A., 2006. Torghabeh Mesozonal Orogenic (pyrrhotite, pyrite, arsenopyrite) Gold Deposit, Formed in Shear Zones Within Ilmenite-type Granitoid Rocks. Iran. Journal of Geosciences 15, 130-141.

Karimpour M.H. and Sadeghi M., 2019. A new hypothesis on parameters controlling the formation and size of porphyry copper deposits: Implications on thermal gradient of subducted oceanic slab, depth of dehydration and partial melting along the Kerman copper belt in Iran. Ore Geology Reviews 104, 522-539.

Karimpour M.H., 2005. Comparison of Qale-Zari Cu-Au-Ag deposit with other Iron Oxides Cu-Au (IOGC-Type) deposits and a new classification, Iranian society of crystallography and mineralogy 13, 203-222.

Karimpour M.H., Heidarian Shahri M.H., Malekzadeh Shafaroudi A., Askari A., 2006. Petrology of plutonic rocks, alteration, investigation of special element, fluid inclusions, and geophysical studies in Hired gold mineralization, research and exploration center for ore deposits of Eastern Iran, 261 pp.

Karimpour M.H., Malekzadeh Shafaroudi A., Mazloumi Bajestani A., Schader R.K., Stern C.R., Farmer L., Sadeghi M., 2017. Geochemistry, geochronology, isotope and fluid inclusion studies of the Kuh-Zar deposit, Khaf-Kashmar-Bardaskan magmatic belt, NE Iran: Evidence of gold-rich iron oxide-copper-gold deposit. Journal of Geochemical Exploration 183, 58-78.

Karimpour M.H., Malekzadeh Shafaroudi A., Mohammad F., Askari A., Sadeghi M., Santos J.F., Stern C.R., 2021. Comparison of petrological and geochemical characteristics of three different types of Eocene copper-gold mineralization in eastern Iran, Ore Geology Reviews 138, 104335.

Karimpour M.H., Stern C.R., Farmer G.L., 2010. Zircon U-Pb geochronology, Sr-Nd isotope analyses, and petrogenetic study of the Dehnow diorite and Kuhsangi granodiorite (Paleo-Tethys), NE Iran, Journal of Asian Earth Sciences 37, 384-393.

Karimpour M.H., Zaw Kh., Huston D.L., 2005. S-C-O Isotopes, Fluid Inclusion Microthermometry, and the Genesis of Ore Bearing Fluids at Qale-Zari Fe-Oxide Cu-Au-Ag Mine, Iran, Journal of Sciences 16, 153-168.

Karimzadeh Somarin A., 2006. Geology and geochemistry of the Mendejin plutonicrocks, Mianeh, Iran. Journal of Asian Earth Sciences 27, 819-834.

Kepezhinskas P.K., McDermott F., Defant M.J., Hochstaedter F.G., Drummond M.S., Hawkesworth C.J., Koloskov A., Maury R.C., Bellon H., 1997. Trace element and Sr-Nd-Pb isotopic constraints on a three-component model of Kamchatka arc petrogenesis. Geochimica et Cosmochimica Acta 61, 577-600.

Kluyver H.M., Griffts R.J., Tirrul R., Chance P.N., Meixner H.M., 1978. Geological Quadrangle Map Sheet Lakar Kuh Quadrangle 1:250, 000. Geological Survey of Iran.

Kouhestani H., Ghaderi M., Chang Z., Zaw K., 2015. Constraints on the ore fluids in the Chah Zard breccia-hosted epithermal Au-Ag deposit, west-central Iran: Fluid inclusions and stable isotope data. Ore Geology Reviews 65, 512-521.

Kouhestani H., Ghaderi M., Large R.R., Zaw K., 2017. Texture and chemistry of pyrite at Chah Zard epithermal gold-silver deposit, Iran. Ore Geology Reviews, 84, 80-101.

Kouhestani H., Ghaderi M., Zaw K., Meffre S., Emami M.H., 2012. Geological setting and timing of the Chah Zard breccia-hosted epithermal gold-silver deposit in the Tethyan belt of Iran. Mineralium Deposita 47, 425-440.

Kouhestani H., Mokhtari M.A.A., Chang Z., 2022. Fluid

inclusion and stable isotope constraints on the genesis of epithermal base metal veins in the Armaqan Khaneh mining district, Tarom-Hashtjin metallogenic belt, NW Iran. Australian Journal of Earth Sciences, In press.

Kouhestani H., Mokhtari M.A.A., Chang Z., Johnson A.C., 2018. Intermediate sulfidation type base metal mineralization at Aliabad-Khanchy, Tarom-Hashtjin metallogenic belt, NW Iran. Ore Geology Reviews 93, 1-18.

Kouhestani H., Mokhtari M.A.A., Qin K.Z., Zhang X.N., 2020. Genesis of the Abbasabad epithermal base metal deposit, NW Iran: Evidences from ore geology, fluid inclusion and O-S isotopes. Ore Geology Reviews 126, 103752.

Kouhestani H., Mokhtari M.A.A., Qin K.Z., Zhao J.X., 2019. Fluid inclusion and stable isotope constraints on ore genesis of the Zajkan epithermal base metal deposit, Tarom-Hashtjin metallogenic belt, NW Iran. Ore Geology Reviews 109, 564-584.

Kouhestani H., Mokhtari M.A.A., Qin K.Z., Zhao J.X., 2019. Origin and evolution of hydrothermal fluids in the Marshoun epithermal Pb-Zn-Cu (Ag) deposit, Tarom-Hashtjin metallogenic belt, NW Iran. Ore Geology Reviews 113, 103087.

Kouhestani H., Rastad E., Rashidnejad Omran N., 2008. Auriferous sulfides from the Chah-Bagh gold occurrence, Muteh mining district. Journal of Sciences, Islamic Republic of Iran, University of Tehran 19, 125-136.

Kouhestani H., Rastad E., Rashidnejad Omran N., Mohajjel M., Goldfarb R.J., Ghaderi M., 2014. Orogenic gold mineralization at the Chah Bagh deposit, Muteh gold district, Iran. Journal of Asian Earth Sciences 91, 89-106.

Linnen R.L., Samson I.M., Williams-Jonse A.E, Chakhmouradian A.R., 2014. Geochemistry of the rare-earth element, Nb, Ta, Hf, and Zr deposits. Treatise on Geochemistry. 21, 543-568.

Lindenberg H.G., Groler K., Jacobshagen V., Ibbeken H., 1984. Post-Paleozoic stratigraphy, structure and orogenetic evolution of the southern Sabzevar zone and the Taknar block, Neues Jahrbach for Geologie und Palaontologie, Abhhandlungen, 168, 287-326.

Ma L., Jiang S., Hou M., Dai B., Jiang Y., Yang T., Zhao K., Wie P., Zhu Z., Xu B., 2014. Geochemistry of early cretaceous calc-alkaline lamprophyres in the Jiaodong Peninsula: Implication for lithospheric evolution of the eastern North China craton. Gondwana research 25, 859-872.

Maghsoudi A., Rahmani M., Rashidi B., 2005. Gold deposites and indications of iran. Res. Man. Students Earth sciences.

Mahdavi P. and Gorabjipour A., 2002. Overviwe of the status of gold, Iran ministry of industeries and mines, Geological survey, National data base on earth science, 67 p. (In persian).

Malekzadeh Shafaroudi A., Karimpour M.H., Stern C.R., 2012. Zircon U-Pb dating of Maherabad porphyry copper-gold prospect area: evidence for a late Eocene porphyry- related metallogenic epoch in east of Iran. Economic Geology 3, 41-60 (in Persian with English abstract).

Mazloumi A., Karimpour M.H., Rassa I., Rahimi B, Vosoughi Abedini M., 2008. Kuh-Zar gold deposit in Torbat-e-Heydaryeh, New Model of Gold Mineralization, Iranian society of crystallography and mineralogy 16, 363-376.

Mazloumi A.R. and Rassa I., 2009. Alteration and petrology of Intrusive Rocks associated with gold mineralization at Kuh-Zar gold deposit, Torbat-e-Heydaryeh, Journal of economic geology of Iran 1, 57-69.

McCulloch M.T. and Bennett V.C., 1994. Progressive growth of the Earth's continental-crust and depleted mantle: Geochemical constraints. Geochimica et Cosmochimica Acta 58, 4717-4738.

McCulloch M.T., Kyser T.K., Woodhead J.D., Kinsley L., 1994. Pb-Sr-Nd-O isotopic constraints on the origin of rhyolites from the Taupo volcanic zone of New Zealand: Evidence for assimilation followed by fractionation of basalt. Contributions to Mineralogy and Petrology 115, 303-312.

Mclnnes B.I.A., Evans N.J., Belousova E., Griffin W.T., Andrew R.L., 2003. Timing of mineralization and exhumation processes at the Sar Cheshmeh and Meiduk porphyry Cu deposits, Kerman belt, Iran. In: Eliopoulos et al. (Eds.). Mineral Exploration and Sustainable De- velopment. 7th Biennial SGA Meeting, Athens, August 24-28. Mill- press, Rotterdam, 1197-1120.

Mehrabi B., Yardley B.W.D., Cam J.R., 1999. Sediment-hosted disseminated gold mineralization at Zarshuran, NW Iran. Mineralium Deposita 34, 673-696.

Miranvari A.S., Calagari A., Siahcheshm K., Sohrabi G., 2019. Investigation of genesis and fluid origin in Noghduz gold bearing quartz veins, East Azarbaijan Province, northwest of Iran. Iranian Journal of crystallography and mineralogy 27, 551-564.

Mohammadi F., 2006. Termometry, petrography and geochemistry of alteration zones in Qale-Zari copper-gold mine, M.S. thesis, Ferdowsi university of Mashhad, 237 pp.

Nezafati N., 2006. Au-Sn-W-Cu-Mineralization in the Astaneh-Sarband Area, West Central Iran, including a comparison of the ores with ancient bronze artifacts from Western Asia. PhD thesis, University of Tb0069006e00670065n.

Nekouvaght Tak M.A., 2008. Magmatism and metallogeny of the Astaneh -Nezam Abad area, Sanandaj -Sirjan Zone, west central Iran. [PhD thesis] University of Clausthl, Germany.

Omidianfar S., Monsef I., Rahgoshay M., Zheng J., Cousens B., 2020. The middle Eocene high-K magmatism in Eastern Iran Magmatic Belt: constraints from U-Pb zircon geochronology and Sr-Nd isotopic ratios. International Geology Review 62, 1751-1768.

Pearce J.A., 1983. Role of the sub-continental lithosphere in magma genesis at active continental margins. In: Hawkesworth, C.J., Norry, M.J. (Eds.): Continental basalts and mantle xenoliths, Nantwich, United Kingdom. Shiva Publisher, 230-249.

Pearce J.A., Harris N.B.W., Tindle A.G., 1984. Trace element

discrimination diagrams for the tectonic interpretation of granitic rocks. Journal of Petrology 25, 956-983.

Pirajno F., 2009. Hydrothermal Processes and Mineral System. Springer, Australia, 1273 pp.

Ramezani J. and Tucker R.D., 2003. The Saghand region, central Iran, U-Pb geochronology, petrogenesis and implications for Gondwana tectonics, American Journal of Science 303, 622-665.

Rashid Nejad-Omran N., Emami H., Sabzehei M., Rastad E., Bellon H., Pique' A., 2002. Lithostratigraphie et histoire pale'ozoe'que a' pale'oce'ne des complexes me'tamorphiques de la re'gion de Muteh, zone de Sanandaj-Sirjan (Iran me'ridonal). 334 C.R. Geoscience 1185-1191.

Rastad E., Monazami Miralipour A., Moumenzadeh M., 2002. Sheikh-Ali copper deposit, A cyprus- type vms deposit in southeast Iran, Journal of sciences Islamic Republic of Iran 13, 51-63.

Richards J.P., Spell T., Rameh E., Razique A., Fletcher T., 2012. High Sr/Y magmas reflect arc maturity, high magmatic water content, and porphyry Cu ± Mo ± Au potential: examples from the Tethyan arcs of central and eastern Iran and western Pakistan. Economic Geology 107, 295-332.

Richards J.P., 2003, Metallogeny of the neo-Tethys arc in central Iran, in Eliopoulos et al., Eds., Mineral exploration and sustainable development: Rotterdam. Millpress, 1237-1239.

Rollinson H., 1993. Using Geochemical Data: Evaluation, Presentation, Interpretation. Longman Scientific and Technical, London.

Rudnick R.L., 1995. Making continental crust. Nature 378, 571-578.

Samiee S., Karimpour M.H., Ghaderi M., Haidarian Shahri M.R., Kloetzli U., Santos J.F., 2016. Petrogenesis of sub-volcanic rocks from the Khunik prospecting area, south of Birjand, Iran: Geochemical, Sr-Nd isotopic and U-Pb zircon constraints" Journal of Asian Earth Sciences 115, 170-182.

Samiee S., 2015. Mineralization, Petrology and geophysic studies in Khunik area, South of Birjand, PhD thesis, Ferdowsi university of Mashhad, 268 pp.

Samiee S. and Zirjanizadeh S., 2019. Geology, mineralogy and geochemistry of Koodakan 2 prospecting area, South of Birjand, East of Lut Block. Journal of Economic Geology 11, 339-355.

Shabani K., Nezafati. N., Momenzadeh M., Rassa I., 2010. Geology, Geochemistry and Mineralogy of the Tareek Darreh gold Deposit, Northeast Iran, Geología Colombiana 35, 131-142.

Shafiei B. and Shahabpour J., 2008. Gold distribution in porphyry copper deposits of Kerman region, Southeastern Iran. Journal of Sciences, Islamic Republic of Iran 19, 247-260.

Shamanian G.H., Hedenquist J.W., Hattori K.H., Hassanzadeh J., 2004. The Gandy and Abolhassani epithermal prospects in the Alborz Magmatic Arc, Semnan Province, Northern Iran. Economic Geology 99, 691-712.

Sun S.S. and McDonough W.F., 1989. Chemical and isotopic systematics of oceanic basalts: Implications for mantle composition and processes. Geological Society Special Publication 42, 313-345.

Taylor H.P., 1978. Oxygen and hydrogen isotopic studies of plutonic granitic rocks, Earth and Planetary Science Letters 38, 177-210.

Taylor S.R. and McLennan S.M., 1985. The Continental Crust: Its Composition and Evolution" Blackwell Scientific publication, Oxford, 312 p.

Torabian A., 2004 .Petrography, mineralogy, geochemistry and fluid inclusion studies of Torghabeh Gold Deposit, M.S. thesis, Ferdowsi University of Mashhad, 30 pp.

Vervoort J.D., Patchett P.J., Blichert- Toft J., Albarede F., 1999. Relationship between Lu- Hf and Sm-Nd isotopic systems in the global sedimentary system, Earth and Planetary Science Letters 168, 79-99.

Wilson M., 1989. Igneous Petrogenesis. A Global Tectonic Approach, Harper Collins Academic, London, 466 pp.

Winter J.D., 2001. An Introduction to Igneous and Metamorphic Petrology. Prentice Hall Inc., Upper Saddle River, 697 pp.

Yuichi S., Ogawa K., Akiyama N., 1976. Copper ores from Qale-Zari mine, Iran. Mining Geology 26, 385-391.

Zarasvandi A., Liaghat S., Zentilli M., 2010. Geology of the Darreh-Zerreshk and Ali-Abad Porphyry Copper Deposits, Central Iran, International Geology Review 47, 620-646.